

# PROJECT FINAL REPORT

**Grant Agreement number: 228933**

**Project acronym: VIBRANT**

**Project title: in Vivo Imaging of Betacell Receptors by Applied NanoTechnology**

**Funding Scheme:IP**

**Period covered: from 01.07.2009 to 31.6.2013**

**Name of the scientific representative of the project's co-ordinator<sup>1</sup>, Title and Organisation:**

**Theo Schotten Ph.D., CAN GmbH, Hamburg, Germany**

**Tel: +49(0)40-42838-8214**

**Fax: +49(0)40-42838-5797**

**E-mail: ts@can-hamburg.de**

**Project website address: [www.fp7-vibrant.eu](http://www.fp7-vibrant.eu)**

---

<sup>1</sup> Usually the contact person of the coordinator as specified in Art. 8.1. of the Grant Agreement.

## 4.1 Final publishable summary report

The publishable summary includes **5 distinct parts** described below:

- An executive summary (1 page).
- A summary description of project context and objectives (4 pages).
- A description of the main S&T results/foregrounds (25 pages),
- The potential impact (including the socio-economic impact and the wider societal implications of the project so far) and the main dissemination activities and exploitation of results (not exceeding 10 pages).
- The address of the project public website, if applicable as well as relevant contact details.

## 1. Executive summary

# VIBRANT

[www.fp7-vibrant.eu](http://www.fp7-vibrant.eu)

### *In Vivo Imaging of **Beta-cell Receptors** by Applied Nano Technology*

Currently, around 30 million people in the enlarged Europe suffer from diabetes, with a prevalence of 7.5% in the member states. By 2025, the number of people with diabetes is expected to rise to around 50 million in Europe, thus increasing prevalence to 10.9%. This devastating disease is ranked among the leading causes of fatal cardiovascular diseases, kidney failure, neuropathy, lower limb amputation and blindness. Estimates of annual direct costs of diabetes care in Europe are currently EUR 50 billion. The indirect costs of diabetes i.e. the costs of lost production are as high as the direct costs or even higher, not to speak of the intangible suffering of the patients and their families.

Diabetes results from an absolute or relative decline in pancreatic  $\beta$ -cell function and/or mass. Studies suggest that gradual loss of  $\beta$ -cell mass (BCM) starts many years before the disease becomes overt. Therefore, non-invasive *in-vivo* imaging and quantification of BCM is of ultimate importance for diabetes management and the development of novel therapies. Unfortunately, such diagnostic methods hitherto do not exist.

The principal goal of VIBRANT is the development of nano-technology-based magnetic resonance imaging (MRI) agents for diabetes diagnosis. The two major objectives of VIBRANT are

1. to develop a method suitable for the non-invasive imaging and quantification of insulin-producing  $\beta$ -cells in the pancreas of diabetic human subjects by means of target specific nanoparticulate probes, and
2. to study the beneficial or adverse effects of ligand functionalized nanoparticulate probes for potential therapeutic applications, e.g. targeted drug delivery systems.

In VIBRANT, a biocompatible, non-toxic polymeric nanocontainer containing a sensitive - optionally multimodal- reporter system or therapeutic agents was accomplished *via* highly reproducible microfluidic processes. The nanocapsules showed low unspecific binding, superior sensitivity and longitudinal signal stability in MRI and optical readouts (T1, T2\*,  $^{19}\text{F}$ , fluorescent). The outer surface of this nanocapsule was decorated with various recognition motifs for the *in vivo* targeting of the pancreatic  $\beta$ -cell. Substantial progress has been accomplished in *in vivo* imaging of functional  $\beta$ -cell mass and a novel *ex vivo* mesoscopic optical imaging (OPT/SPIM) provided exact cross-validation of prelabeled islet transplants in the pancreas. However, all recognition motifs tested for  $\beta$ -cell specific binding showed insufficient target affinity; hence determination of  $\beta$ -cell mass after systemic administration of labeled nanocontainers needs future improvements.

## 2. VIBRANT Summary Description

The increasing global incidence of diabetes and the tremendous socio-economical impact of the disease and its sequels urgently demands for major improvements in preventive medicine, early diagnosis and therapy. Studies suggest that one of the main causations of diabetes, namely the gradual deterioration of pancreatic  $\beta$ -cell mass (BCM), precedes overt diabetes for more than a decade. In order to find a remedy against these deficiencies, the principal goal of VIBRANT was the development of nano-technology-based magnetic resonance imaging (MRI) agents for early diabetes diagnosis by determination of BCM.

To this end, VIBRANT was constituted around a consortium of nine renowned European research institutions and one SME in the fields of diabetology,  $\beta$ -cell physiology, imaging and nanotechnology.

Name	Short name	Country
Center for Applied Nanotechnology (CAN) GmbH (Coordinator)	CAN	Germany
Dept. of Chemistry, Univ. Hamburg	UH	Germany
Rolf Luft Research Center for Diabetes and Endocrinology, Karolinska Institutet, Stockholm	KI	Sweden
Laboratory of Experimental Hormonology, Brussels Free University	ULB	Belgium
Centre for Molecular Medicine, Umeå University	UMU	Sweden
Centre for Genomic Regulation, Barcelona	CRG	Spain
Katholieke Universiteit Leuven	K.U.Leuven	Belgium
Centre for Biomolecular Interactions Bremen	UniHB	Germany
Universität Bayreuth	UBT	Germany
University of Copenhagen	UCPH	Denmark

The two major objectives of VIBRANT were:

1. to develop a method suitable for the non-invasive imaging and quantification of insulin-producing  $\beta$ -cells in the pancreas of diabetic human subjects by means of target specific nanoparticulate probes,

and

2. to study the beneficial or adverse effects of ligand functionalized nanoparticulate probes for potential therapeutic applications, e.g. targeted drug delivery systems.

Two anatomical features of the pancreas demand for technical solutions, far more advanced than those required for other imaging applications. First,  $\beta$ -cells exist in tiny (100–300  $\mu\text{m}$  in diameter) micro-organs, the islets of Langerhans, which are distributed throughout the exocrine pancreas. Each is too small to be spatially resolved by current non-invasive *in vivo* imaging methods. Second, the total  $\beta$ -cell mass, even in healthy humans, is so small (about 1 g) as to constitute only about 1–2% of the total pancreatic mass.

This required

- i. a contrast agent providing a stable and high signal intensity,
- ii. a contrast agent that is highly specific to the cell type, but devoid of toxicity, and
- iii. an imaging technology with the potential of paramount spatial resolution.

For a more comprehensive knowledge about  $\beta$ -cell functionality with regard to proliferation and apoptosis, in order to eventually stall  $\beta$ -cell deterioration and induce increase of functional BCM, an agent would be desirable, which

- iv. allows monitoring of functional aspects (viability status of the  $\beta$ -cell)
- v. holds the potential for a novel  $\beta$ -cell specific drug delivery system

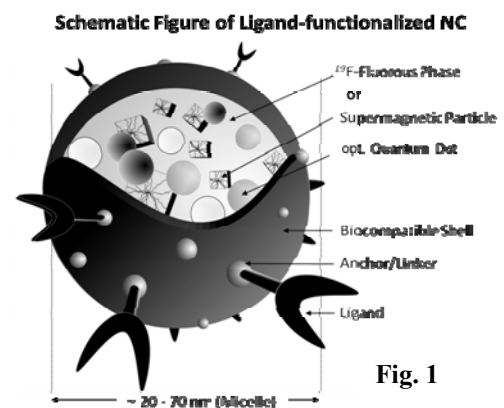
In order to address these objectives, VIBRANT aimed for novel MRI contrast agents, which provide sufficient sensitivity and spatial resolution power, as well as the potential for quantification. Magnetic resonance imaging (MRI) as a diagnostic tool, offers numerous advantages, e.g. high spatial resolution, potential of functional imaging, and lack of radiation exposure (suitable for screening). Superparamagnetic iron oxide nanoparticles (SPIONs) offer high sensitivity and spatial resolution, whereas novel  $^{19}\text{F}$ -containing imaging agents hold the potential of quantification. Furthermore, the hyperintense contrast of the  $^{19}\text{F}$  signal holds the potential to avoid the common problem of hypointense artifacts and to image the contrasted structures in absence of anatomical background. For this purpose, VIBRANT envisioned micellar nanocontainers comprised of amphiphilic polymers micelles, enclosing optionally superparamagnetic nanoparticles or fluorinated agents and –optionally - fluorescent quantum dots (QD) suitable for a cross-validation by multiplex read-out. The magneto-fluorescent interdependencies of the constituents were studied, adverse interferences were minimized and the potential of this multi-component system optimized. In summary, a **first result** of VIBRANT are **Nano-Containers (NCs)**, which stably enclose superparamagnetic nanoparticles ( $\text{Fe}_2\text{O}_3$ ,  $\text{Fe}_3\text{O}_4$ ) or fluororous phases for high sensitivity/high resolution MRI, optionally together with fluorescent quantum dots.

The outer shell of the nanocontainers is comprised of biocompatible polymer chains, amenable to functionalization with biomolecules (antibodies, carbohydrates or peptides). The latter were used in order to achieve affinity and specificity to insulin secreting cells (see Fig. 1).

In summary, the **second result** of VIBRANT is the fully fledged technology for the preparation of diverse ligand functionalized NCs.

A plethora of variations in size, shape, payload, linker chemistries and geometries, as well as ligands, ligand density or surface coverage of the nanocontainer were prepared and tested, which pivotally determined the biological properties. In VIBRANT a cascade of cell assays was used in order to optimize the ligand functionalized FPNC with regard to biocompatibility, lack of toxicity, affinity and specificity. In particular, the effects on  $\beta$ -cell function, survival and regeneration was investigated *in vitro* by analyzing various functional parameters of insulin secreting cells, like glucose utilization, glucose oxidation, mitochondrial membrane potential, insulin release, and apoptosis. In summary, the **third result** of VIBRANT are biocompatible, non-toxic nanoconstructs, which did not affect cellular viability and metabolism and show moderate to high affinity as well as selectivity for insulin secreting cells *in vitro*, suitable for further *in vivo* testing.

In VIBRANT, a globally unique *in vivo* anterior chamber model (ACE) of the eye was utilized, thus directly exploring the effects of the nanoconstructs on fully vascularized and innervated islet transplants.<sup>1</sup> The optimized ligand functionalized NCs finally were tested *in vivo* on islet transplants, as well as in type 1 and type 2 diabetes models, in order to differentiate and quantify  $\beta$ -cell mass of healthy vs. impaired pancreata using confocal



microscopy and MRI. Unfortunately –despite of a careful selection of the most state-of-the-art assays and models- VIBRANT encountered a common issue in drug research, i.e. that the *in vitro* results only partially translated into *in vivo* models. In particular, the NC constructs, identified in cellular tests showed insufficient labeling of islets *in vivo*. Nevertheless, a novel small molecule carbohydrate derivative, **AJ070** -not in the primary scope of VIBRANT- showed promising results *in vitro* and *in vivo* and will be pursued further.

Modified NCs comprised of a biodegradable polymer shell were studied for their potential as drug delivery systems in order to restore, maintain or improve *in vivo*  $\beta$ -cell function. First evidence for the feasibility of this approach was gained. In summary, **a fourth result** of VIBRANT is the demonstration of the potential of this concept to diagnostic and therapeutic applications *in vivo*.

It was planned to cross-validate and calibrate the results by an independent method, - optical projection tomography (OPT). This novel *ex vivo* imaging technology offers unprecedented power for 3D whole-organ imaging, but with a resolution approaching the cellular scale. Within VIBRANT, this unique technology was further improved and optimized. Because of insufficient effectivity of ligand functionalized NCs *in vivo*, surrogate studies were performed demonstrating the feasibility of the concept for *in vivo* BCM imaging and quantification in type 1 and type 2 diabetes disease models. In summary, **a fifth result** of VIBRANT is the independent cross-validation and confirmation of MRI results by OPT in a proof-of-principle study.

In summary, **a sixth result** of VIBRANT is the consolidation of the developed nanoparticular agents, processes and associated methodology in view of comprehensive IP protection, the dissemination to the scientific community and the societal stakeholders, and the commercialization of nanoparticular components (e.g. STREM Chemicals Inc.). Three patent applications were filed, besides 56 peer-reviewed research publications, about 80 conference contributions, and 7 articles and interviews to the general public. An Industrial Advisory Board (IAB) associated to VIBRANT (Servier, Lilly, BMS/Amylin and JDRF) will facilitate uptake after the end of VIBRANT for follow-up cooperations with partners from the pharmaceutical industry.

## Overall strategy

The VIBRANT workplan was structured in the form of **four major strategic segments** (see Figure 2), which combine in a comprehensive framework and corresponded to the major development phases of the value chain in the project:

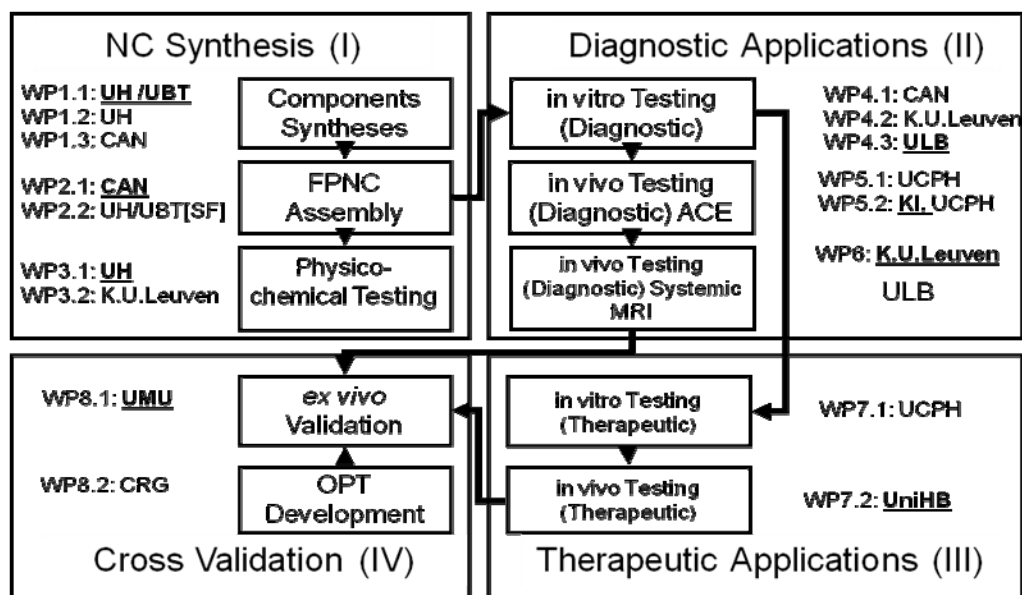


Fig. 2:  
VIBRANT  
PERT Chart  
Overview

As a basis and starting point of the project work, the **first segment (I)** consisting of WPs 1 to 3, addressed all aspects in context with the synthesis of novel ligand functionalized nanocontainers. As a result, ligand functionalized NCs, containing  $^{19}\text{F}$  or superparamagnetic MRI contrast agents, optionally combined with fluorescent QDs, as well as the associated technology to produce, characterize and iteratively optimize these constructs were provided.

The **second segment (II)**, WP 4 to 6, built on segment I, pursuing the testing and optimization of ligand functionalized NCs with regard to  $\beta$ -cell specific targeting, sensitivity, spatial resolution, toxicity, signal stability, and potential quantification for diagnostic non-invasive *in vivo* imaging of the pancreas. As a result, stable, nontoxic NCs with high sensitivity and high spatial resolution power for imaging were provided, demonstrating  $\beta$ -cell specificity *in vitro*. However, translation of these findings into *in vivo* was not fully conclusive.

The **third segment (III)**, consisting of WP 7, leveraged on the observations made in part (II) in order to explore ligand functionalized NCs as vehicles for the targeted delivery of therapeutics to the pancreatic  $\beta$ -cell. A robust 3D MR imaging of the mouse abdomen was developed for the analysis of  $\beta$ -cell function/ mass and measurement techniques of the mouse abdomen with manganese in two animal models of diabetes. Targeting of  $\beta$ -cell survival and function *in vivo* was studied. As a result, first evidence that drug-loaded nanocontainers specifically support pro-survival in  $\beta$ -cells was gained.

The **fourth segment (IV)** incorporated in WP 8, concluded the development work by providing an independent *ex vivo* cross validation of the *in vivo* experiments of part (II) and (III) using innovative OPT and SPIM technology. Due to the lack of functional NCs *in vivo*, surrogate studies were performed in MRI in such a way that labeled islets were grafted into pancreata and cross validated with OPT. As a result, precise superimposition of islet grafts and 3D quantification of BCM was demonstrated by optimized correlation and calibration algorithms. Additionally, novel correlative OPT/SPIM and near infrared OPT (NIR-OPT) instruments with increased multichannel capacities were engineered.

**In summary, VIBRANT provided comprehensive technology for the manufacturing of nanoparticulate probes, bearing biological recognition motifs, for multi-modal imaging and drug-delivery. Superparamagnetic iron oxide NCs were highly sensitive for the detection of single islets and superior to commercial materials. The fluorine phase MRI agents developed, offer new opportunities for improved imaging modalities.**

**Knowledge on  $\beta$ -cell function, survival and regeneration was substantially expanded. During VIBRANT, highly sophisticated *in vitro* assays and *in vivo* models were developed and adapted to MRI. An independent cross-validation of the MRI results was accomplished by OPT.  $\text{Mn}^{2+}$ -enhanced MRI can detect small changes in functional  $\beta$ -cells *in vivo* and is a potential method for early noninvasive detection of changes in functional  $\beta$ -cell mass.**

Unfortunately, -at the time- *in vivo*  $\beta$ -cell imaging by means of nanoparticulate probes was not achievable, possibly due to insufficient  $\beta$ -cell affinity of the selected ligands. However, search for novel high-affinity ligands was not in the scope of VIBRANT. Once as such will become available, studies should be resumed, because all technical success factors have been developed. In particular, surrogate proof-of-principle studies clearly indicate feasibility of anatomical and functional pancreatic  $\beta$ -cell imaging and quantification of BCM. Promisingly, a small molecule fluorescent carbohydrate derivative AJ 070 showed specific labeling of islets *in vitro* and *in vivo* and will be further pursued.

### 3. VIBRANT main S&T results/foregrounds

#### WP 1 Component Synthesis

In workpackage 1 (WP 1) all necessary components, like superparamagnetic or fluorescent nanoparticles, a range of biocompatible polymers for encapsulation, various fluororous phases for fluorine ( $^{19}\text{F}$ )-MRI, carbohydrate and proteinogenic bioligands for affinity labeling have been provided.

#### WP 1.1 Particle synthesis

*Quantum dots:* The highly fluorescent quantum dots used in VIBRANT were made using an innovative continuous flow reactor<sup>2</sup>.

Compared to the common “batch” synthesis, this process leads to superior reproducibility of the particle properties with significance lower than 0.1%. Figure 1.1 shows absorption and emission measurements of three different batches of quantum dots.

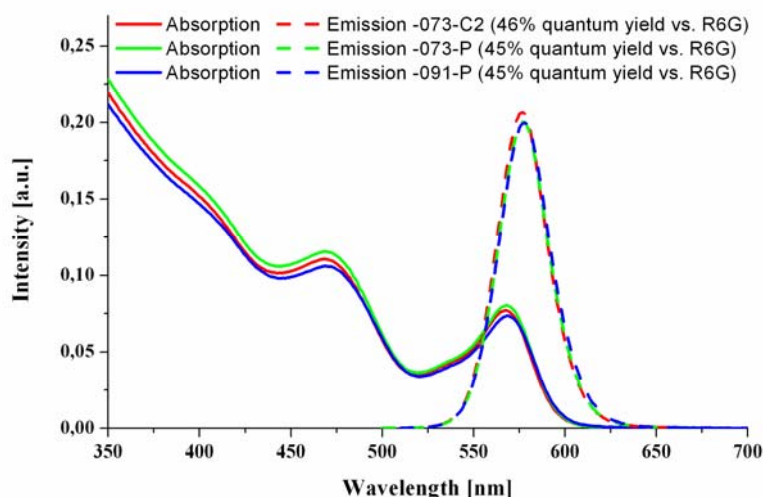


Figure 1.1: Absorption and emission spectra of three different batches of quantum dots

Fluorescence and stability were improved by growing CdS and ZnS shells around the CdSe cores. Absorption and emission spectra of CdSe/CdS/ZnS particles can be tuned between 550 and 625 nm. The quantum yields are usually above 40%.

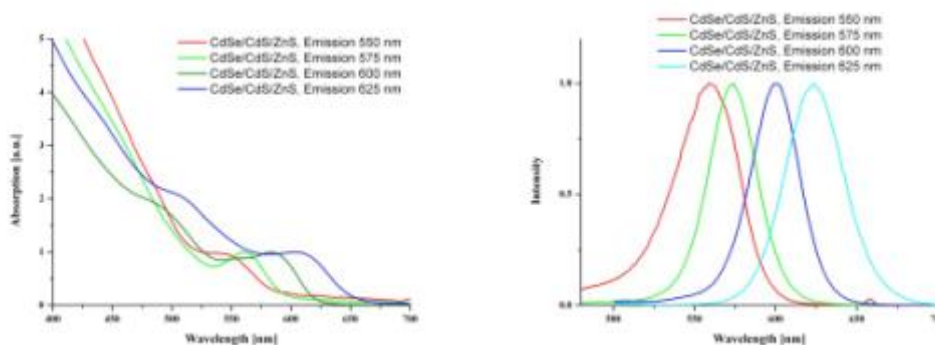


Figure 1.2: absorption and emission spectra of CdSe/CdS/ZnS particles



Recently, these materials were commercialized under the trademark CANdots® Series A<sup>3</sup> and distributed by STREM Chemicals<sup>4</sup>.

#### *Iron oxide:*

The superparamagnetic iron oxide nanoparticles (SPIOs) used within VIBRANT were produced with diameters between 4 and 20 nm and a narrow distribution smaller than 10%. Alternatively, continuous flow synthesis of SPIOs of different sizes was successful, albeit size distribution still leaves room for improvements.

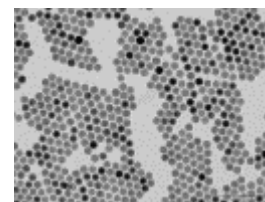


Fig. 1.3 SPIOs

### WP 1.2 Polymers

For biological applications, the hydrophobic inorganic nanoparticles synthesized as described above need to be encapsulated into a biocompatible polymer shell in order to render the particles water soluble. To this end, so-called amphiphilic diblock copolymers, comprised of a threadlike hydrophobic and a hydrophilic block each were used. In water, these polymers self-assemble to spherical micelles enclosing the nanoparticle in the center (see WP2). The hydrophobic blocks adhere to the nanoparticle surface, wherein the hydrophilic blocks point outwards to the aqueous environment, hence rendering this nanocontainer water soluble. The synthesis and properties of these amphiphilic polymers are described herein.

The hydrophilic block of all block copolymers consisted of polyethylene glycol (PEG), in combination with different hydrophobic blocks, namely poly lactic acid (PLA), poly caprolactone (PCL), poly caprolactone-co-glycolide PCLGL, or poly isoprene (PI). All block copolymers were synthesized by sequential living anionic polymerization and/or coordination-insertion polymerization, hence providing narrow dispersity and good control over molecular weight. Typical examples of poly(lactid acid-*b*-ethylene glycol) (PLA-PEG), poly(caprolactone-*b*-ethylene glycol) (PCL-PEG) and poly(isoprene-*b*-ethylene glycol) (PI-PEG) are shown in Fig. 1.4

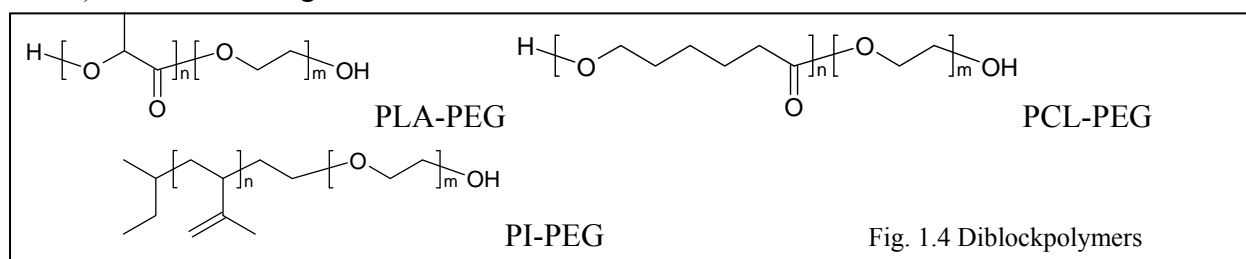


Fig. 1.4 Diblockpolymers

The PEG-terminal OH-group was converted into terminal amino, isocyanate, alkynyl and carboxylic acid groups by standard functional group transformations for subsequent conjugation with biotin, carbohydrates, peptides, antibodies, or other putative β-cell specific ligands.

Additionally, for <sup>19</sup>F-MRI the standard diblock polymers were perfluorinated at the hydrophobic terminus. However, signal intensity was insufficient. In contrast, encapsulation of monomeric F-phases, e.g. perfluorooctyl bromide (PFOB), perfluoro-15-crown-5-ether, or perfluorohexyl octane (F6H8) provided satisfying signals (see WP3). Advantageously, most monomeric F-phases (PFOB, F6H8) are clinically approved.

### WP 1.3 Carbohydrate Ligands

Specific labeling of pancreatic  $\beta$ -cells is extremely challenging, because of the scarcity of  $\beta$ -cell specific targets, e.g. receptors etc. In VIBRANT numerous potential targets from the literature were studied for their suitability. In particular, it was reported that streptozotocin (STZ)<sup>5</sup> as well as mannoheptulose<sup>6</sup> and their derivatives show selectivity for the GLUT2 transporter of  $\beta$ -cells. Accordingly, various series of optionally fluorinated *gluco*- or *manno*-heptulose derivatives were synthesized, with linkers for the straightforward conjugation to the nanocontainers.

These derivatives either resemble the (desnitroso) urea pharmacophore of the STZ, or a glycosidic bond (Fig.1.5).

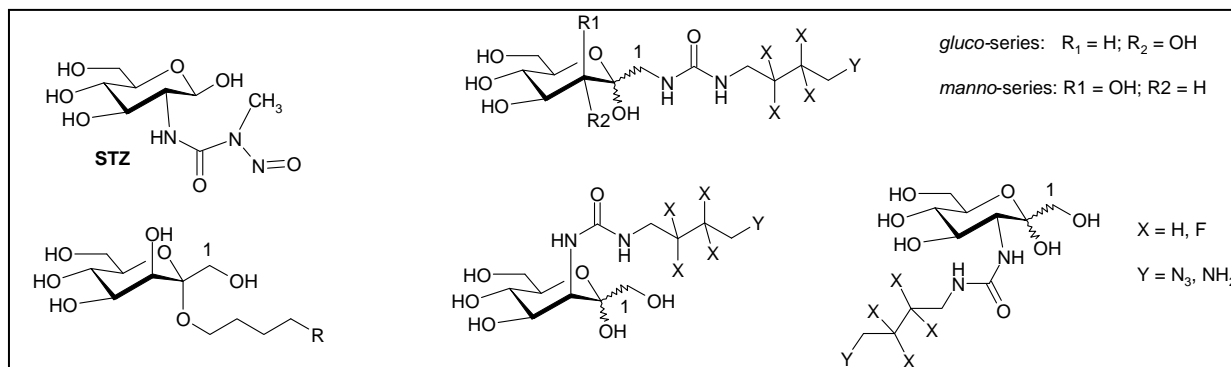


**Fig. 1.5:** STZ and heptulose derivatives

Additionally, regioisomeric F-heptuloses were synthesized and successfully tested in MRI (*in vitro* and *in vivo*). Notably, a non-toxic fluorescent mannoheptuloside **AJ070** showed significant binding to islets (*in vitro* and *in vivo*). A novel SPR-based assay for surface analysis of glycosylated NPs revealed strong cooperative binding effects ( $K_D$  200.000 higher than for monomeric saccharides).

### WP 1.4 Proteinogenic Affinity Ligands

Within VIBRANT, two antibodies, namely GLUT2ab and the recently described  $\beta$ -cell specific single chain antibody SCA B5<sup>7</sup>, as well as various GLP-1 peptide derivatives were procured for conjugation to nanocontainers and subsequent biological testing. In a first optimization cycle a uniform conjugation protocol was chosen based on the well-known biotin/NeutrAvidin dyad. Commercially available biotinylated GLUT2 antibody was selected for proof of principle experiments, because within the pancreas, GLUT2 is exclusively expressed in  $\beta$ -cells. The full length antibody was chosen for benchmarking, temporarily ignoring potential immunogenicity and putative co-expression of GLUT2 in adjacent tissues like liver, kidney and the small intestine. Direct covalent, as well as biotin/NeutrAvidin conjugation was accomplished. As an additional target, a recently published single-chain antibody SCA B5, claiming high  $\beta$ -cell specificity was chosen. To this end, the construction of an 8x-histidine, thrombin cleavage site and biotin AviTag labeled version of the published SCA B5 amino acid sequence was achieved.

## WP 2: Nanocontainer Assembly

According to the VIBRANT workplan, in WP2 all components procured in WP1 were assembled to a functional nanocontainer. This requires the phase transfer of the hydrophobic nanoparticle, e.g. fluorescent quantum dots (QD) or super-paramagnetic iron oxide

nanoparticles (SPIO) or liquid fluorous phase from the organic phase into water, as well as bio-conjugation to the affinity ligand. A standard operation procedure (SOP) was developed, using a continuous flow phase transfer process, which provides highly reproducible nanocontainers with hydrodynamic diameter in the range of 30 to 120 nm at comparably high production volumes. A subsequent purification step removed by-products or empty micelles. Numerous series of fluorinated and non-fluorinated micellar NCs have been prepared using different methodologies, offering optimized solutions for either diagnostic (contrast agent) or therapeutic (controlled release) applications.

Nanocontainers comprised of polymers containing carbon-carbon double bonds, like PI-*b*-PEG, offer the option of radical induced crosslinking, thus providing exceptionally stable nanocontainers. Evidently, crosslinked NCs offer benefits e.g. increased circulation half live and longitudinal signal stability for imaging, whereas crosslinking is rather detrimental for controlled release. For the latter, nanocontainers comprised of biodegradable polyester-*b*-PEG polymers, mainly poly(lactic acid-*b*-ethylene glycol) (PLA-PEG) and poly(caprolactone-*b*-ethylene glycol) (PCL-PEG), were developed (Fig. 2.1).

Polymer Shell		Fluorous Phase	
PI-DETA/PI-PEO	Contrast Agent	PFOB (monomer)	
PS/PI-PEO		PF-15-crown-5 /opt. w/F6H8 (monomer)	
PCL-PEO	Controlled Release	R <sub>F</sub> -PCL-PEO-X (polymer)	
PLA-PEO		R <sub>F</sub> -PLA-PEO-X (polymer)	
PBCA		R <sub>F</sub> -PEO-X (polymer)	

**Fig. 2.1:** Optimized polymer shells for contrast agents or drug delivery

All polymers in use were biocompatible and functionalization was achievable by various methods (see below). For diagnostic applications, highly fluorescent quantum dots (QDs) and superparamagnetic iron oxide nanoparticles (SPIONs), as well as monomeric F-phases were optionally co-encapsulated into FPNCs or non-fluorinated NCs. With regard to fluorinated nanocontainers, only monomeric F-phases provided sufficient NMR/MRI signal (see WP3). However, polymeric F-phases, e.g. R<sub>F</sub>-PCL-PEO-X, R<sub>F</sub>-PLA-PEO-X or R<sub>F</sub>-PEO-X, strongly facilitated solubilization of monomeric F-phases.

Three different methodologies for the assembly and functionalization of the nanocontainers were developed (Fig 2.2 and Fig. 2.3):

### 1. Post-Assembly

A nanocontainer is formed in a first step and functionalized with a bio-ligand thereafter

### 2. Pre-Assembly

A polymer chain is functionalized with a bio-ligand and subsequently assembled to a nanocontainer

### 3. Seeded emulsion polymerisation (SEP) with “*in situ*” functionalization

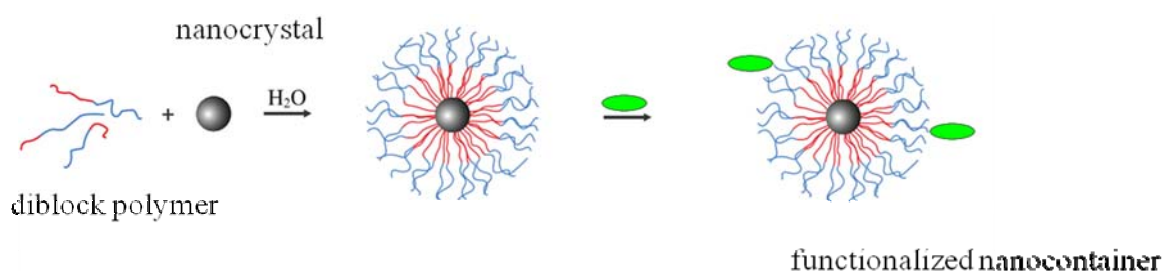
A mixture of matrix monomers and tethered (bio)-ligands were co-polymerized around nanoparticles, hence forming (bio)-functionalized nanocontainers in a single step<sup>8</sup>

The “**post-assembly**” approach was preferred for delicate affinity ligands, e.g. antibodies, which were conjugated to the full-fledged nanocontainer *via* biotin/Neutravidin, or *via* amino- or carboxy groups using conventional bioconjugation methodologies. However, the

conjugation yield and ligand density on the surface of the NC was difficult to control and to analyze.

The “**pre-assembly**” strategy offered better control of the surface coverage of affinity ligands on the NC by employing defined mixtures of functionalized and unfunctionalized polymers. This approach was well suited for robust small molecules, e.g. pyranoses or biotin, which are sufficiently soluble in the required organic solvents and compatible with reaction conditions, like radical induced cross-linking and elevated temperatures. Furthermore, structural elucidation of the affinity molecule polymer conjugate by standard spectroscopy (e.g. NMR) prior to the assembly was usually possible, whereas these methods, when applied to a full-fledged NC, generally failed.

### “Post-Assembly”



### “Pre-Assembly”

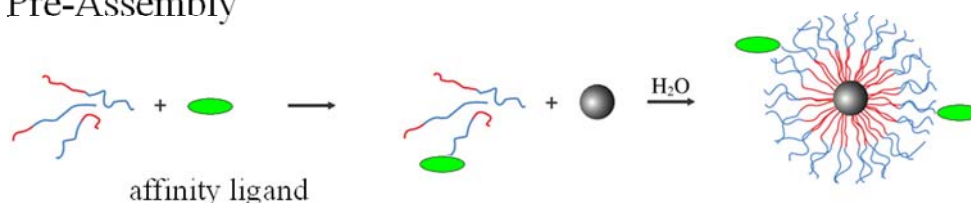


**Fig. 2.2:** Assembly strategies

Alternatively, using **seeded emulsion polymerisation (SEP) with “in situ” functionalization** by transferring hydrophobic nanoparticles into water, using surfmers (i.e. polymerizable surfactants) and adding variable mixtures of matrix forming monomers, e.g. styrene or divinyl benzene in combination with bioligands attached to a polymerizable tether, provided excellent results in a single polymerization step (*vide infra*).

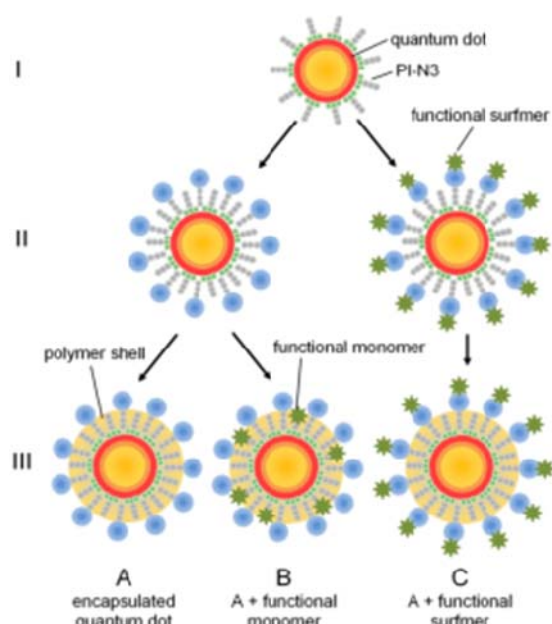
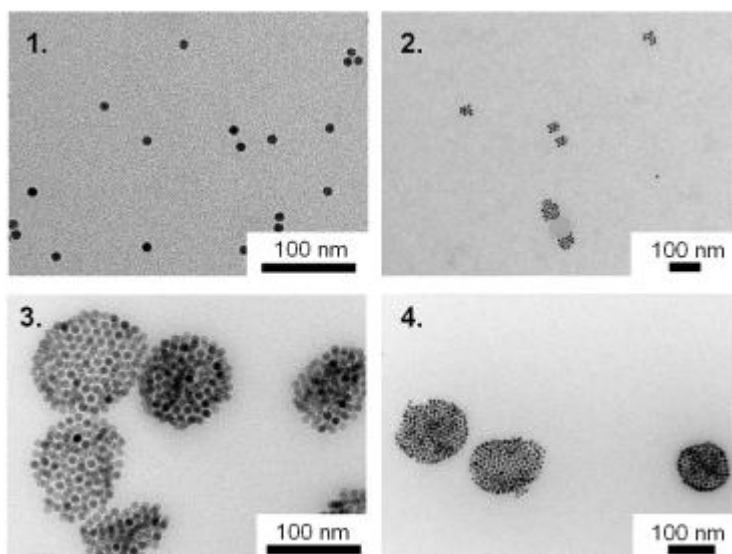


**Fig. 2.3:** Encapsulation of QDs by SEP: I) PI-N3 coated QD; II) QD in PI-b-PEO micelle after phase transfer; III) QD encapsulated in polystyrene: A) without additional functionality; B) with copolymerized functional monomer; C) with functional surfmer.

The continuous flow phase transfer process developed within VIBRANT, not only allows precise tuning of the NCs’ size distribution and surface coverage, but also provides control over the numbers of nanoparticles enclosed. Hence, by tuning the process parameters, e.g. absolute and relative concentrations of the components or the geometries of the mixing chamber, all kinds of NCs, either bearing a singular nanocrystal, or enclosing a large number of nanocrystals were

deliberately accomplished. Clustering of nanocrystals offers advantages, either by clustering different e.g. fluorescent and superparamagnetic nanocrystals providing hybrids for multichannel read-outs, or by clustering solely superparamagnetic nanocrystals for optimal MRI contrast (Fig. 2.4, see WP3)

**Fig. 2.4:** TEM images of single and clustered 9.8 nm SPIONs. The size bar is equivalent with 100 nm. Determined  $d_{\text{hyd}}$  by DLS measurements were 59 nm (1.), 73 nm (2.), 126 nm (3.), and 132 nm (4.).



However, the increased hydrodynamic diameter of the clusters has to be considered with respect to the biological properties, e.g. passing biological barriers (see WP5). Overall, within VIBRANT, more than 100 diverse nanocontainers were prepared, physico-chemically characterized and subsequently tested in a staggered panel of biological assays.

### WP 3: Physico-chemical Characterization

In WP 3 the diverse series of nanocontainers (NCs) prepared in WP 2, were characterized by spectroscopic, electron microscopic and magnetic analytical methods. Furthermore, NCs were evaluated and optimized with regard to their suitability as contrast agents for cellular imaging.

#### **<sup>19</sup>F-MRI contrast media**

Initially, two series of PLA/PCL-PEG block copolymers with terminal perfluorinated appendages or perfluorinated blocks (e.g. R<sub>F</sub>-PCL-PEO-X and R<sub>F</sub>-PLA-PEO-X, see WP1) were successfully synthesized and used for the preparation of stable micelles with a hydrodynamic diameter of about 50 nm (WP 2). However, both series of micellar FPNCs gave no usable <sup>19</sup>F signals, assumedly to the restricted motility of polymer-bound F-atoms.

In contrast, encapsulation of monomeric F-phases, e.g. perfluoro octyl bromide (Perflubron®, PFOB) or perfluoro-15-crown-5-ether (CellSense®, PF-15-c5) succeeded in stable micelles providing high sensitivity in <sup>19</sup>F-MRI. The detectability limit of at least 5 x 10<sup>15</sup> equivalent <sup>19</sup>F atoms per voxel was established with the help of radio-frequency coils especially developed within VIBRANT (see also WP6). In particular, the PFOB containing PI-PEO micelles showed good stability within a tuneable hydrodynamic diameter of 30 to 110 nm, depending on the PFOB content. However, PFOB displays a multi-signal <sup>19</sup>F NMR spectrum, due to non-equivalent F-atoms. Thus “ghosts”, i.e. several images of the same object, were detected in <sup>19</sup>F MRI, provided that the usual large bandwidth of 8000Hz was used. Elimination of these ghosting artefacts succeeded, by using selective excitation pulses with a reduced bandwidth of 1000Hz.

Favourably, PF-15-c5 contains 20 equivalent F-atoms, thus providing a singlet, most suitable for MRI. Routine encapsulation with PI-*b*-PEG initially failed, but eventually was successful by using the partially fluorinated polymers R<sub>F</sub>-PCL-PEO-X and R<sub>F</sub>-PLA-PEO-X, or by means



of a semi fluorinated solubilizer perfluorohexyl octane (F6H8). Quantification of the  $^{19}\text{F}$ -MRI signal was achieved by comparison with an external standard (e.g. calibration with a 5-fluoro cytosine or NaF solution).

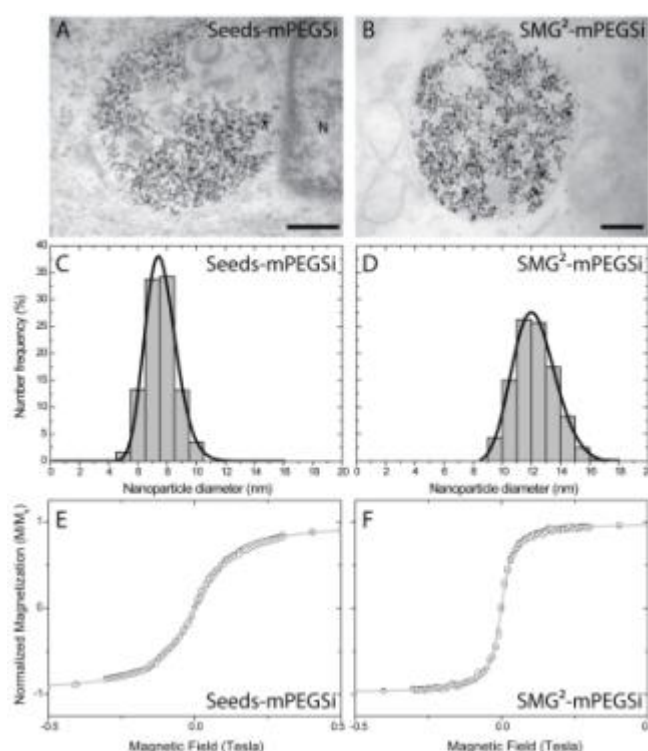
Additionally, libraries of fluorinated mannoheptulose and glucoheptulose derivatives were synthesized (WP 1) and their cellular uptake in hepatocytes, INS-1 cells and pancreatic islets was studied (WP 4)<sup>9</sup>. Cell labeling with intracellular concentrations of up to 20mM (up to  $10^{12}$   $^{19}\text{F}$  per cell) of fluoro sugars was sufficient for MR imaging. The detectability of labeled cells was considerably improved by using custom build radio-frequency coils (detectability limit 20,000 cell  $\mu\text{l}^{-1}$ ).  $^{19}\text{F}$ -labelled mannoheptuloses showed high specificity to the GLUT2-transporter, thus suggesting their utility as novel imaging agents.<sup>10</sup>

### Iron oxide contrast media (SPIOs)

Iron oxide containing contrast agents were assessed to confirm their size, size distribution (monodispersity), magnetic properties and potential clustering using TEM, dynamic light scattering, determination of the blocking temperature, squid, MRI and EPR (see Figure 3.1). For better uptake/ binding, quantification, sensitivity and biocompatibility, it was our aim to obtain monodisperse, superparamagnetic particles with high T2 relaxivity. Iron oxide based particles developed in VIBRANT were superior to commercially available particles in all aspects.

In order to further optimize the already near perfect MR contrast, we assessed the dependency of MR contrast on the size of nanoparticles. Hereby, we used PEGylated iron oxide based particles and magnetoliposomes synthesized *via* the seed-mediated growth method, providing mono-disperse particles of different sizes. As can be seen, the larger particles obtained after two seed-mediated growth steps showed superior MRI properties compared to the original seed particles (Fig. 3.1, right column).

**Fig. 3.1:** (A),(B) Bright field TEM images and (C),(D) corresponding histograms of Seed-mPEGSi (A),(C), and SMG<sup>2</sup>-mPEGSi (B),(D). Scale bar of the TEM images is 200 nm. The histograms, plotted as diameter versus number frequency, were fitted with a lognormal curve. (E),(F) Normalized magnetic hysteresis curves of Seed-mPEGSi (E) and SMG<sup>2</sup>-mPEGSi (F) measured at 300 K. The grey curves are the corresponding Langevin curve fits.



Due to the intracellular degradation of the outer phospholipid bilayer of magnetoliposomes (ML), MLs are prone to intracellular clustering. This was confirmed by experiments that compared PEG-silane coated particles with MLs of the same core. Comparison of MR contrast of cells labelled initially with the same amount of iron oxide particles showed that MLs resulted in stronger contrast and contained particles for a longer time.

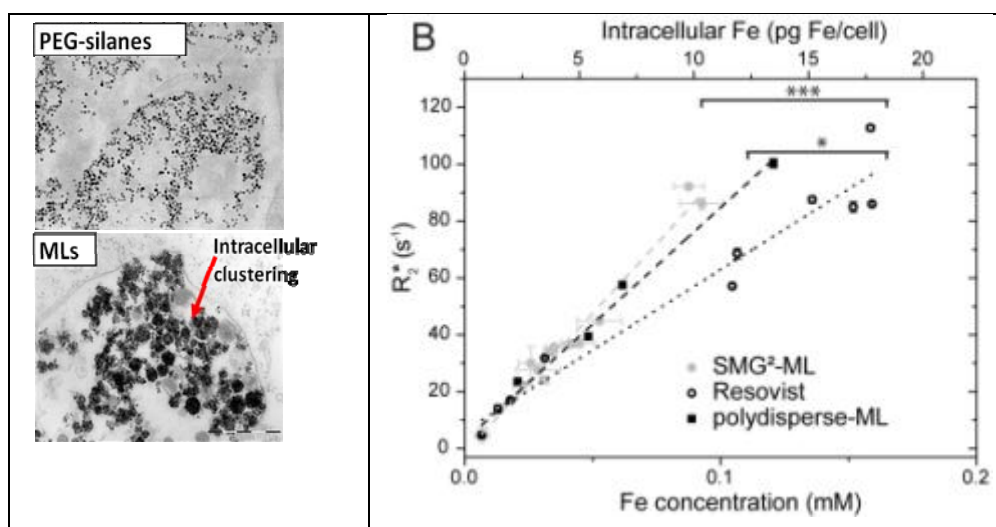


**Fig. 3.2:** TEM images of PEG-silanes and MLs taken up by MSCs confirm the intracellular clustering of MLs, which contributes to their better MR contrast and longitudinal in vivo monitoring. (B) Clustered MLs provide a better MR contrast as confirmed by relaxivity measurements.

In order to transfer the beneficial effects of clustering to biofunctionalized NCs, seeded emulsion polymerization (SEP), as described in WP2 was used, providing biofunctionalizable SPIO clusters with precisely defined properties (Fig 3.3).

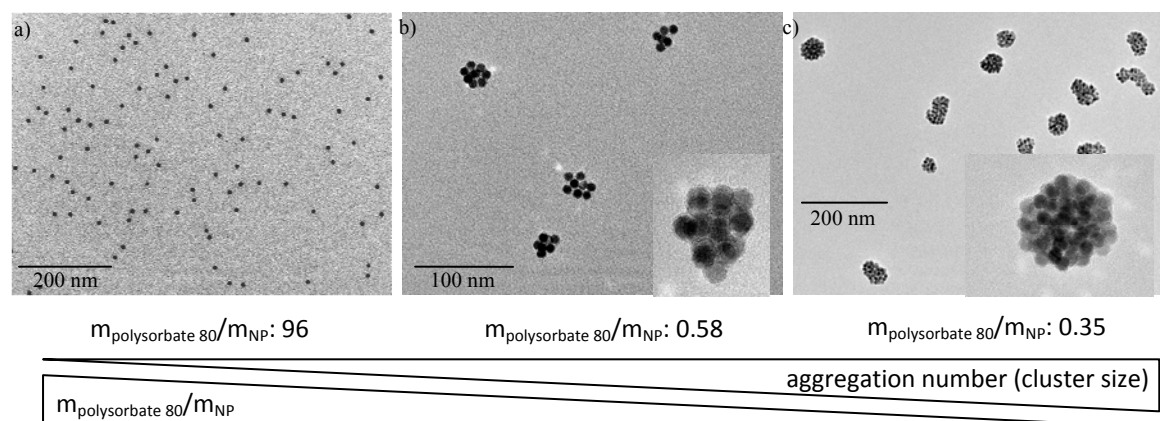


**Fig. 3.3:** Clustering of SPIOs by seeded emulsion polymerisation.

### Fluorescent contrast media (QDs)

Application of seeded emulsion polymerization (SEP) to the encapsulation of fluorescent quantum dots (QDs) provided nanocontainers (NCs) with remarkably improved stability against various reagents, e.g. metal ions, EDTA, aldehydes etc. which may be used in the preparation of biological specimens<sup>11</sup>. This was a major progress, inevitable for the crossvalidation studies (WP8).

### Hybrid contrast media

For multimodal read-out, as required for the crossvalidation studies of WP8, binary combinations of the foregoing described contrast media were tested. Again, the newly developed SEP process provided excellent results.

### Magneto-fluorescent nanocontainers: QD/SPIO hybrids

The main challenge of hybridisation is to minimize mutual adverse effects of different nanoparticles, e.g. to prevent fluorescence quenching of QDs by the release of iron ions from SPIOs.

As can be seen in Fig. 3.5, SEP of spherical SPIOs and longitudinal quantum dot rods provided hybrids (A) preserving all properties of the disparate particles (B,C,D)

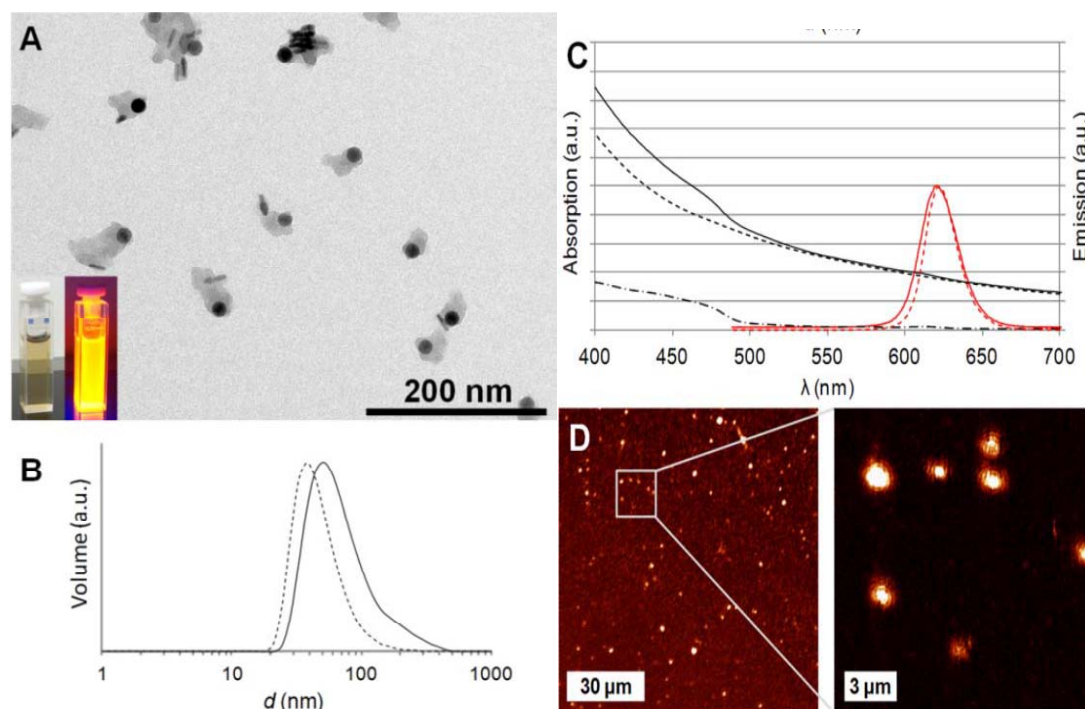


**Fig. 3.5:** A: TEM image of the QDQR iron oxide hybrids (inlay: hybrids under room light (left) and under UV light (right)); B: DLS histograms of the hybrids (volume distribution) of the encapsulated iron oxide particles before (dashed line) and after hybrid formation (solid line); C: black: absorption spectra of the hybrids (solid line), polystyrene encapsulated iron oxide nanocrystals (dashed line), QDQRs (dot dashed line); red: normalized emission spectra of the hybrids (solid line) and QDQRs solely (dashed line); D: confocal fluorescence microscopy images of the hybrids.

### Fluorous phase-fluorescent nanocontainers: $^{19}\text{F}$ /QD hybrids

Co-encapsulation of fluorous phase and QDs was successful. Fluorescence and  $^{19}\text{F}$ -signals were fully maintained without mutual impairment. The size of the NCs was tuneable *via* the fluorous phase/polymer ratio, e.g. at a ratio of 1  $\mu\text{L}$  fluorous phase per mg polymer NC diameter increased to 100nm or higher.

#### $^{19}\text{F}$ /SPIO hybrids

Co-encapsulation of fluorous phase and SPIOs was technically feasible, but the  $^{19}\text{F}$ /SPIO hybrids did not provide any  $^{19}\text{F}$ -signal.

Two series of PI-PEG micelles loaded with PFOB and SPIOs of 10 nm or 6 nm diameters respectively were prepared. In both cases no  $^{19}\text{F}$  MRI-signal could be detected with standard NMR and MRI methods. In further experiments the PFOB/SPIO (10 nm) hybrids were subjected to "pulse-acquire" MR spectroscopy. Excitation was performed with a 10 $\mu\text{s}$  pulse and data were acquired after 2.5  $\mu\text{s}$ . However, by 3  $\mu\text{s}$  complete dephasing of the F-signal occurred. Consequently, further efforts towards  $^{19}\text{F}$ /SPIO hybrids were abandoned.



## WP 4: *In vitro* screening of NCs on cell lines and primary cells

In WP 4 the nanocontainers (NCs) prepared in WP 2 and subsequently characterized in WP 3 were screened in cellular assays, with regard to toxicity, unspecific adhesion,  $\beta$ -cell selectivity and cellular response.

### **Standard toxicity screening of NCs on human lung carcinoma cell line A549**

The initial screen of all NCs was a standard toxicity assay on the human lung carcinoma A549 cell line. Cell viability and integrity were measured *via* WST-1 (water soluble tetrazolium) and LDH (lactate dehydrogenase) assay, respectively. This screening was well suited for the identification of putatively toxic by-products from NC manufacturing. After optimization and standardization of the preparation protocols, all NCs were nontoxic in the relevant concentration range. In particular, concentrations of the NCs up to 0.5  $\mu$ M did not

- reduce cell proliferation or vitality
- cause cell lyses
- show optical/microscopic evidence for cellular changes

Preparations of NCs, which did not pass these criteria, either were purified again or excluded from further testing.

### **Testing NCs for toxicity on INS1 cell line using the xCELLigence platform**

Further development of the NCs for possible *in vivo* applications required in-depth understanding of their effects on  $\beta$ -cells. In particular, in later clinical applications the residual  $\beta$ -cell mass of type 1 or type 2 diabetes patients may be impaired by metabolic and inflammatory stress. Consequently, a high content functional model was required, which preferably maps  $\beta$ -cell biology and allowed screening of NCs on both unchallenged and challenged  $\beta$ -cells and in  $\beta$ -cells exposed to factors that affect  $\beta$ -cell regeneration and replication. This was accomplished by adapting a novel real-time, on-line technology, the xCELLigence cell-analyser platform, offered by Roche. Different insulin producing  $\beta$ -cell lines were tested, from which the INS1 was chosen as mostly suitable, thus establishing a powerful high content screening tool.

Routine screening of NCs typically showed no toxicity up to 250 nM, whereas at 1000 nM all NC were toxic to INS1 cells.

Furthermore, the INS1-xCelligence platform was remarkably sensitive for the detection of toxic byproducts. Even minute amounts of sodium azide, conventionally used for the preservation of NCs against bacterial contamination were detected.

Most notably, a unique profile was screened out for a NC conjugate to GLP1 (EU-0533), which solely showed a proliferative effect at concentrations of up to 100nM. Binding to INS1 cells was proven by fluorescence microscopy (Fig. 4.1).

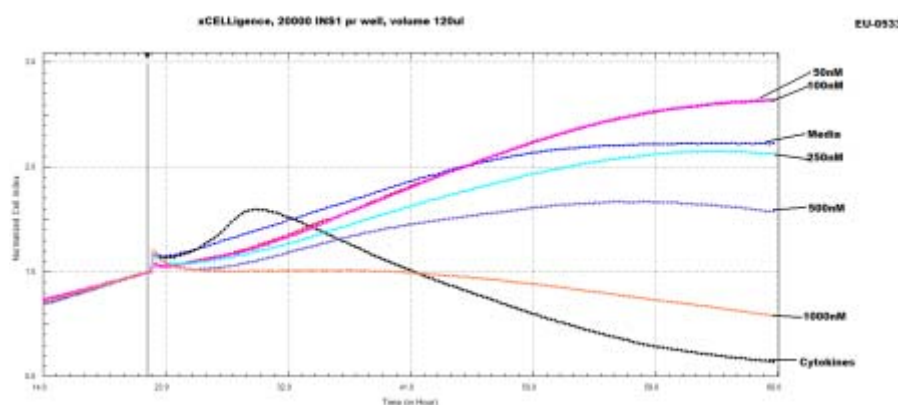


**Fig. 4.1:** Viability of INS1 cells, when exposed to positive and negative controls, as well as EU-0533. 20000 INS1 cells were exposed to medium, cytokines (150 pg/ml IL-1 $\beta$  and 5 ng/ml IFN $\gamma$ ), and the NPs were tested at 50 nM to 1000nM.

## Toxicity screening of NCs on mesenchymal stem cells, MSC and multipotent adult progenitor cells, MAPC

Deriving insulin-expressing cells from Multipotent Adult Progenitor Cells (MAPC), induced pluripotent stem cells (iPSC) and other progenitors would be a major progress for the treatment of diabetes. Unfortunately so far, heterogeneous cell populations were obtained, from which insulin-expressing cells/ $\beta$ -cells are difficult to discriminate. Therefore, NCs were tested for toxicity on these cells, in order to estimate their potential for specific labeling of insulin expressing cells derived from MAPCs. After careful purification, NCs were devoid of toxicity in the relevant concentration range.

## Functional effects of NCs on pancreatic islets

The effects of NCs on glucose-induced insulin secretion were tested on freshly isolated rat islets. The non-targeted nanoparticles only affected adversely insulin release evoked by D-glucose or other nutrient secretagogues when used in high concentrations, i.e. in the 0.5 to 1.0  $\mu$ M range in the case of NC (+ FeOx) and in the 0.3 to 1.0  $\mu$ M range in the case of NC (+ QD). The NC (+ QD) and NC (+ FeOx), even when tested at an 1.0  $\mu$ M concentration, only provoked minor changes in the metabolism in D-glucose (16.7 mM). Likewise, the functionalized nanoparticles all tested at a 50 nM concentration did not alter insulin output and D-glucose metabolism significantly, irrespective of the preparative route (post- vs. pre-assembly) and nanoparticle load (QD or SPIOs).

12

## Cell Adhesion Tests

For reliably imaging of a small cell mass, like pancreatic  $\beta$ -cells, unspecific adhesion or uptake of NCs needs to be minimized.

The PEG-coated unfunctionalized NCs were devoid of unspecific binding to cells in protein supplemented culture media. Unspecific binding was evoked, for NCs providing positive surface charge by protein depletion of the medium. The biotin/NeutrAvidin conjugation strategy for the attachment of the affinity ligands reduced unspecific background to less than 1%, even if incubation was performed in protein free medium. Conjugates obtained directly *via* heterobifunctional linkers were preferably incubated in full medium to reduce background.

In summary, a conjugation system was established that provided nontoxic nanoparticle-affinity molecule conjugates, virtually free of unspecific adhesion.

## Specific binding of ligand functionalized NCs

NC conjugates providing GLUT2 antibody and a GLP-1 derivative proved specific binding on cell culture strains and tissue slides but not on isolated islets.

NC conjugates presenting the anti-GLUT2 antibody exhibited the strongest binding to INS1 cells. However, for the envisioned *in vivo* application putative immunogenicity, as well as co-expression of GLUT2 in adjacent tissues has to be considered. Nevertheless the anti-GLUT2 antibody conjugate was chosen for benchmarking.

The recombinant SCAB5 derivate proved binding to human and rat pancreatic islets in immunohistology experiments and may serve as a backup candidate. Unfortunately, after conjugation to NCs, the construct was dysfunctional.

Exendin-4-NC conjugates showed moderate binding. Notably, the K19-modified GLP-1-NC conjugate **EU 0533** showed intense binding in INS1 cell culture even with short incubation time (10

min), but adversely affected the cells. Surprisingly, in the xCELLigence assay **EU 0533** showed no toxicity, but even improved cell viability compared to the control. Unfortunately, these promising findings at the end of VIBRANT could not be studied in detail anymore (Fig.4.2).

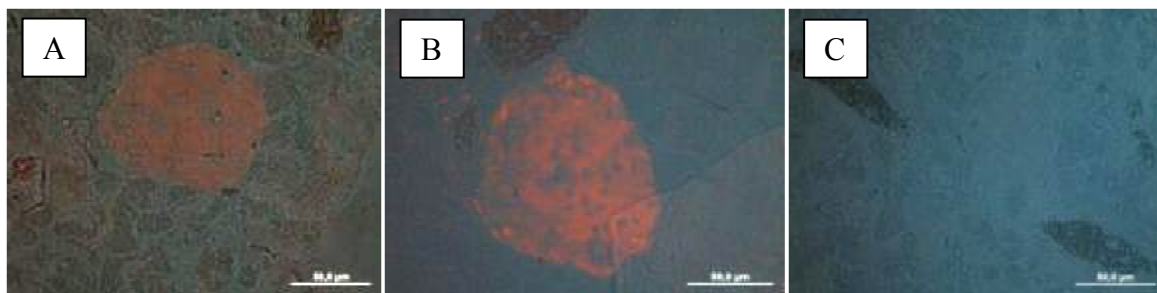


**Fig. 4.2:** Staining of pancreatic islets is clearly visible for the GLUT-2 (A) and KGLP1 (B) probes. Exendin-4 probe did not stain the islets on the slides (C).

Additionally, a fluorescent mannoheptulose conjugate **AJ070**, not in the scope of a nanoparticulate probe, showed accumulation in  $\beta$ -cells *in vitro* and *in vivo* and holds the potential for a novel low molecular weight imaging agent (see WP 5).

In summary, two lead candidates were identified for extensive *in vitro* and *in vivo* evaluation.

## WP 5: *In vivo* Biological Testing in the Anterior Chamber of the Eye (ACE)

One of the main goals of VIBRANT was to develop strategies for the *in vivo* quantification of  $\beta$ -cell mass (BCM), in order to monitor loss or gain of BCM as well as to assess the efficiency of specific therapeutic interventions on BCM. This quantification depends on the development of specific  $\beta$ -cell labeling and detection techniques. This is a challenging task due to the fact that  $\beta$ -cells are deeply embedded in the exocrine pancreas and therefore are difficult to access optically for labeling and functional studies.

When transplanted into the anterior chamber of the eye, pancreatic islets become fully vascularized and innervated. These engrafted islets reflect exactly the status of endogenous islets, thus key aspects of  $\beta$ -cell morphology and function can be studied noninvasively using *in vivo* imaging techniques, due to the ideal optical and structural properties of the eye. The ACE model also offers a unique opportunity to noninvasively detect and visualize fluorescent NCs in islet transplants. In addition to the development of techniques allowing *in vitro* screening of functionalized fluorescent NCs for their specific binding to  $\beta$ -cells, the ACE model permits to assess their potential binding properties under *in vivo* conditions.

### Monitoring loss of BCM

The potential for non-invasively monitoring loss of BCM in the ACE model was clearly demonstrated on islet grafts expressing green fluorescent protein (GFP) in  $\beta$ -cells. Cell death can be visualized by staining with annexin V conjugated to allophycocyanin (APC). If cell death was induced by *i.v.* application of alloxan, the fluorescent staining was strongly increased. Backscatter imaging, which provides structural information about the morphology of endocrine cells, also clearly indicated a diminished BCM.

Loss of BCM was also observed in the BB rat, a model for human type 1 diabetes (T1DM). Genetically, in diabetes-prone (DP) BB strains,  $\beta$ -cell decay and thus onset of diabetes occurs within a narrow, defined time-period, i.e. between 50-70 days of age (Holmberg R. et al., 2011, PNAS 108:10685-9). Diabetes-prone BB rat islets were transplanted into the ACE of DP-BB rats and allowed to vascularize and innervate. Similarly diabetes-resistant BB rat islets were transplanted into the ACE of diabetes-resistant BB rats. FITC-labeled dextran was injected i.v. for the visualization of islet vascularization, backscatter imaging was used to indicate morphological changes of islet grafts. At 100 days of age, islets transplanted into the diabetic BB rats vanished, while islets transplanted into non-diabetic BB controls were still intact and vascularized. Notably, the loss of BCM in the ACE coincided with the onset of diabetes, thus strongly suggesting that the dynamics and changes in BCM imaged in the eye mirror the changes observed in the native islets in the pancreas. Importantly, the loss of BCM can be prevented by treatment of DP-BB rats with antisense-oligonucleotides targeting ApoCIII, which has been identified as one of the T1DM serum factors promoting  $\beta$ -cell death (Holmberg R. et al., 2011, PNAS 108:10685-9). The lowered ApoCIII serum levels prolonged survival of islet grafts and thus delayed onset of T1DM after 93 days vs. 56 days in the non-treated group.

### Monitoring gain of BCM

To monitor changes in BCM we developed a novel image analysis protocol permitting precise quantification of individual islet graft volumes in the anterior chamber of the eye over time. This protocol has been cross-validated by optical projection tomography (OPT), proving that imaging of islet grafts in the eye can successfully report on individual islet volumes and, importantly, on the possible increase or decrease in BCM.

Using this image analysis protocol we successfully reported on the BCM increase occurring in the leptin-deficient ob/ob mouse. This obese mouse is characterized by, among other things, its strong appetite. The increased demand for insulin leads to a quick increase in the number of  $\beta$ -cells in the pancreas, thus to an increase in BCM. We were able to determine that the increase in  $\beta$ -cell mass in the pancreas is reflected by the increase of  $\beta$ -cell mass in the islets engrafted in the anterior chamber of the eye.

Therefore, because islets transplanted in the anterior chamber of the eye reflect endogenous pancreatic islet properties, the ACE model allows for monitoring changes in pancreatic BCM.

### Validating fluorescent molecules for their specific binding to $\beta$ -cells using the ACE

The ACE model serves as a perfect imaging platform allowing for a precise assessment of pancreatic  $\beta$ -cell mass regulation and future validation of functionalized NCs. After *i.v.* administration of fluorescent unfunctionalized NCs (EU0503) we could successfully image the ACE islet graft vasculature *in vivo* via confocal microscopy. This proves that fluorescent compounds can reach the islet graft for assessing their potential binding to  $\beta$ -cells.

We then established an *in vitro* procedure to evaluate binding of functionalized NCs to insulin releasing cells. For validation, cells were incubated with exendin-4 conjugated to a small fluorescent dye. The fluorescence could be detected on mouse islet cells after 2 min incubation at a concentration of 100 nM. Displacement of the fluorescent compound in presence of non-labeled exendin-4 was successful, proving specificity of the ligand binding to islet cells (Fig. 5.1).



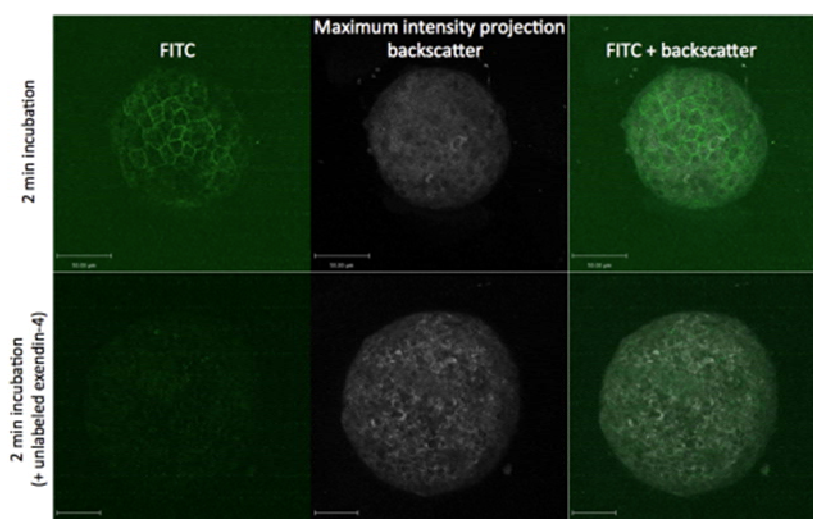


**Fig. 5.1:** *in vitro* binding of exendin-4 conjugated to a small fluorescent dye.

This targeting molecule was then assayed *in vivo* (Figure 5.2) and proved to be suitable both for *in vitro* and *in vivo* specific labeling of islet cells.

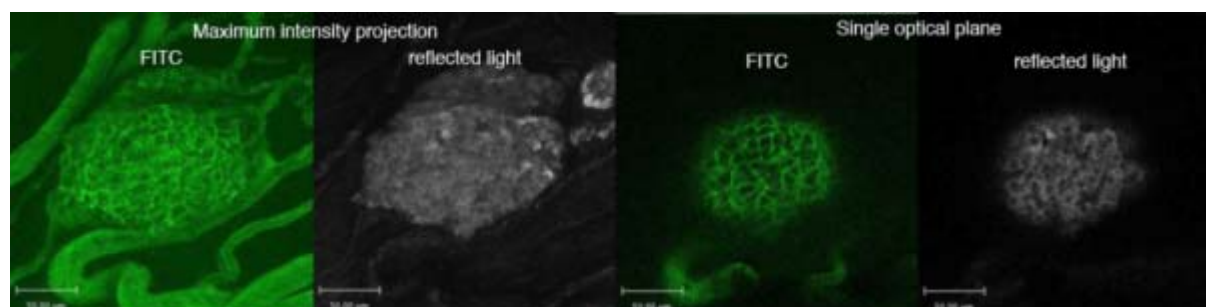


**Fig. 5.2:** *In vivo* imaging of islet transplant, 1 minute after i.v. injection of a fluorescently-labeled exendin-4

We assayed various labeling compounds based on anti-GLUT2, SCAB5 and GLP-1 derivatives, and conjugated either to FITC or to a nanocontainer (NC). Unfortunately none of them proved to exhibit specific binding properties to  $\beta$ -cells (Fig. 5.3). Hence, with the proteinogenic affinity ligands available, no suitable NCs could be identified.

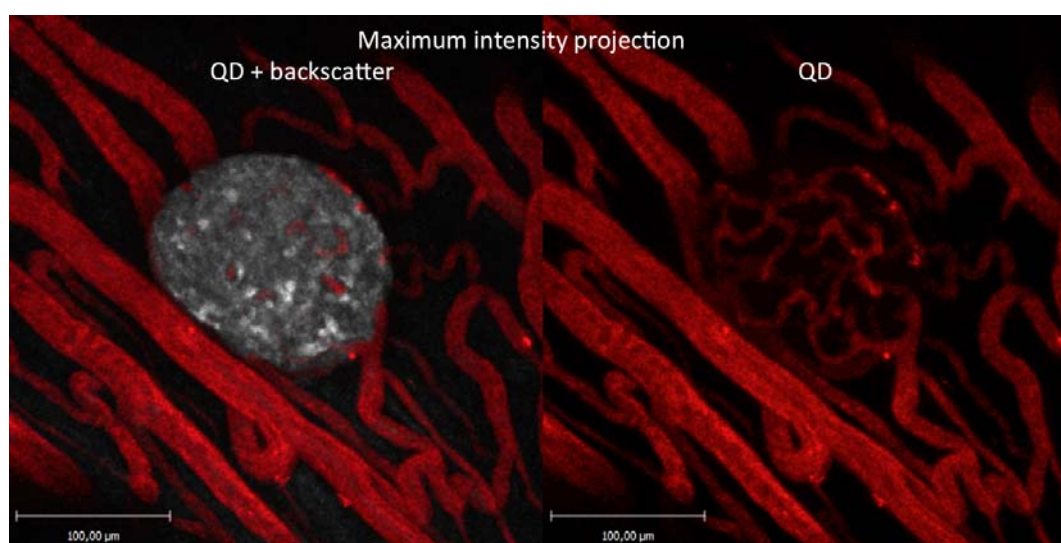


**Fig. 5.3:** *In vivo* imaging of islet transplant 17 minutes after i.v. injection of the SCAB5-labeled NC EU0546. Fluorescence emitted by the quantum dot (QD) enclosed into the NC is shown in red, islet morphology obtained by backscatter imaging is shown in grey. Note that the signal emitted by the QDs remains located in the blood vessels, the NC EU0546 does not show binding to  $\beta$ -cells.

Diverse carbohydrate-modified NCs, in particular desnitroso-STZ conjugates, were tested but none was found to show specific binding to  $\beta$ -cells either. We could however see an accumulation of signal in islet cells using a fluorescent mannoheptulose derivative (AJ070) both *in vitro* and *in vivo* (Fig. 5.4).

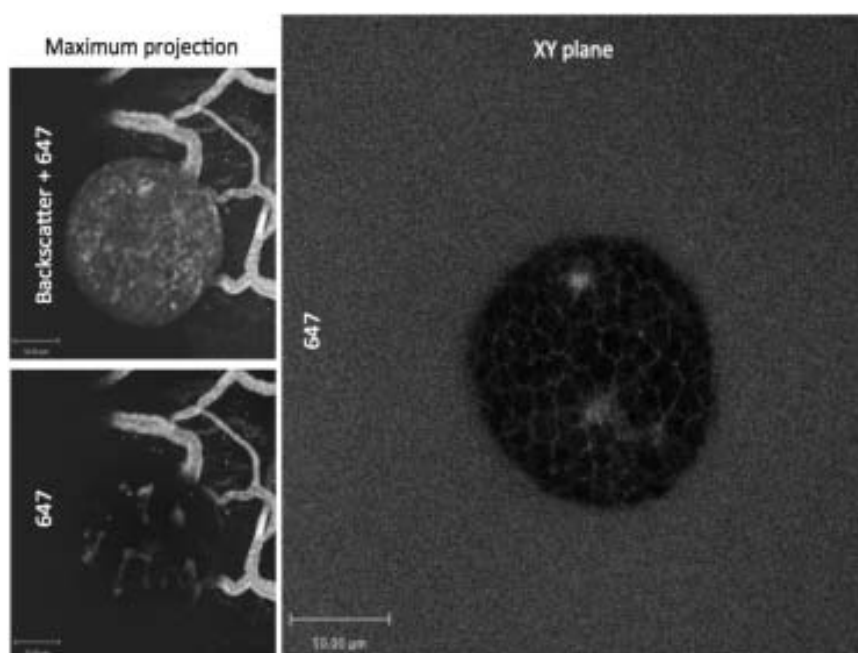


**Fig. 5.4:** *In vivo* imaging of islet transplant after i.v. injection of AJ070

These promising results were achieved at the very end of VIBRANT and will be pursued further in a continued collaboration. In conclusion, we were able to develop and provide a reliable *in vivo* imaging platform for both the assessment of changes in BCM and for screening of compounds targeting specifically  $\beta$ -cells *in vivo*.

## **WP 6 *In vivo* imaging technology**

In WP6 imaging techniques were developed and optimized that allow non-invasive, *in vivo* imaging of pancreatic islets. Hereby, we have focused mainly on magnetic resonance imaging (MRI), which is readily available in the clinic. In addition, *in vivo* optical imaging techniques (mainly fluorescence imaging) were utilized for cross-validation in pre-clinical research.

In order to visualize the FPNCs developed and tested in WP1 to WP4, robust  $^1\text{H}$  and  $^{19}\text{F}$  MRI protocols for imaging the pancreas in experimental models of diabetes and controls were established and exchanged between partners. This includes on one hand the establishment of sensitive and possibly quantitative acquisition protocols but also purpose build hardware components like radio frequency coils for detection of  $^1\text{H}$  and  $^{19}\text{F}$  MR images of the rodent pancreas or the eye for the detection of FPNCs in the anterior chamber model (see WP5).

### **Detection of highly sensitive FPNCs by MRI and fluorescence imaging**

To overcome limitations of individual imaging methods like the low spatial resolution of fluorescence imaging or the lack of absolute quantification of iron oxide based nanoparticles by MRI, bimodal FPNCs were used that target beta cells and contain imaging reporters for fluorescence (for example quantum dots) or MR Imaging (iron oxide based nanoparticles or fluorine containing

compounds). For *in vivo* imaging, iron oxide based particles have proven to be highly sensitive, resulting in the detection of single islets. In combination with quantum dots, unspecific background signal in the MRI can clearly be distinguished from the signals originating from the FPNCs (see also Figure 6.1).

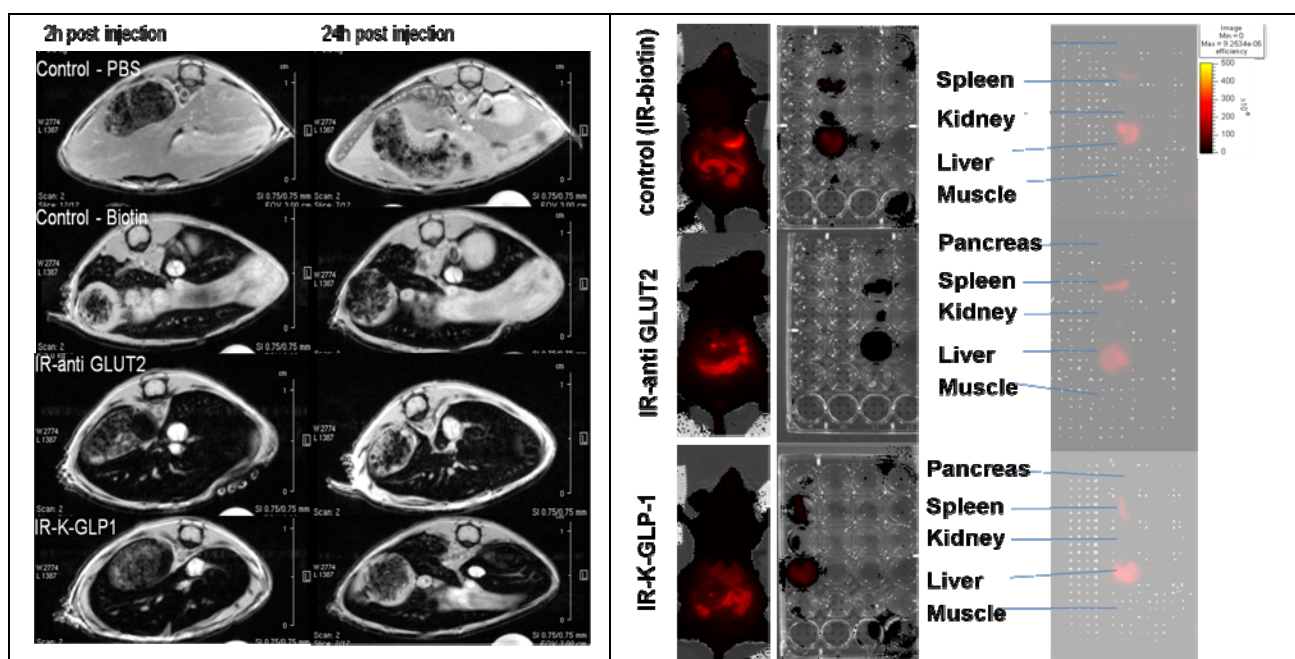


**Figure 6.1:** MR images and *in vivo* fluorescence images of FPNCs developed in the Vibrant project. The particles were functionalized to target GLUT2 (IR-anti GLUT2) or GLP1 (IR-K-GLP1) of the  $\beta$ -cells. Those FPNCs contained iron oxide based nanoparticles and CAndot Series M quantum dots carrying a DyLight 680 labeled neutravidin linker, which was coupled to the respective targeting molecule or just biotin (IR-Biotin) as a control. Particles were systemically injected to test their specificity for  $\beta$ -cells. Imaging was performed repeatedly between 2 to 24 hours after FPNC administration. As seen in the left panel, MR images resulted in a hypointense contrast in the liver, spleen as well as the pancreas region, indicating high sensitivity of the FPNCs. Fluorescence images (right panel) indicates fluorescence signal from the liver, spleen and pancreas region as also confirmed by *ex vivo* fluorescence images. Lack of specificity indicates that particles were also cleared via the spleen and liver.

### Quantitative *in vivo* imaging using fluorine containing compounds and $^{19}\text{F}$ MRI

FNPCs that contained fluorinated compounds (perfluoro carbons, PFC) or small molecules like deoxy-fluoro-mannoheptuloses were tested for their suitability for quantitative *in vivo* assessment of beta cell mass.  $^{19}\text{F}$  MRI proved to be a suitable tool to assess the biodistribution of administered particles *in vivo* with high specificity (no background signal, see Figure 6.2). While PFC containing FPNC proved to be highly sensitive, resulting in the detectability of less than ten islets (see Figure 6.3), deoxy-fluoro-mannoheptuloses showed high specificity to  $\beta$ -cells and were able to reach them under *in vivo* conditions due to the small size of those molecules. However, the sensitivity of deoxy-fluoro-mannoheptuloses based *in vivo* islet detection was insufficient, due to the fact that those molecules contained only one fluorine atom and were cleared from the body relatively quickly. It was possible to quantify the amount of fluorinated compounds and indirectly the amount of cells with *in vivo*  $^{19}\text{F}$  MRI when internal or external standards were applied.



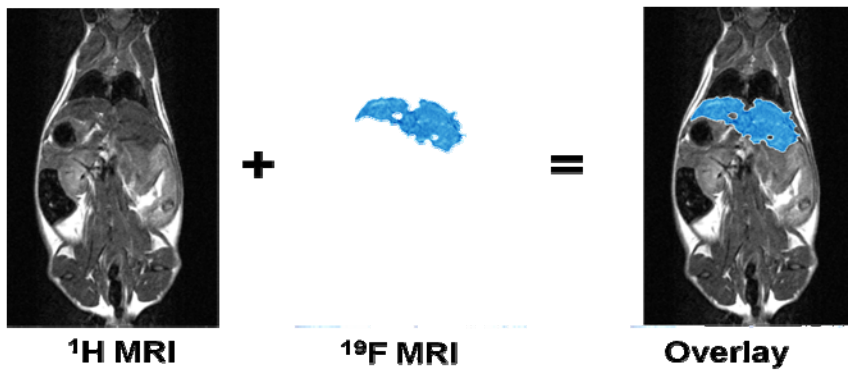


**Figure 6.2:** Biodistribution of PFC containing FNPCs after systemic administration. The  $^{19}\text{F}$  MR image indicates clearance of the FPNCs via the liver. The  $^{19}\text{F}$  MR image indicates high specificity as no background signal was observed. Utilization of purpose build double tuned  $^1\text{H}/^{19}\text{F}$  detectors allows overlay of those  $^{19}\text{F}$  MRI with  $^1\text{H}$  MRI to superimpose anatomical detail.

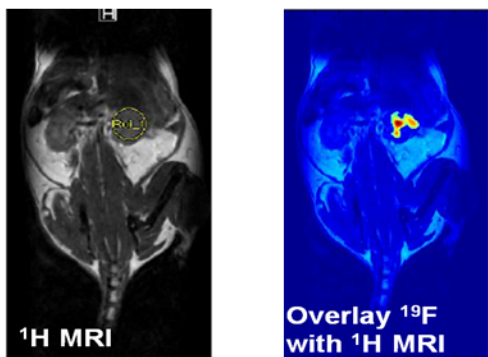


**Figure 6.3:** *In vivo* detection of engrafted pancreatic islets prelabelled with PFCs. The left panel shows an  $^1\text{H}$  MRI, indicating anatomical details in the abdominal cavity. The right panel shows an overlay of  $^1\text{H}$  and  $^{19}\text{F}$  MRI, indicating the location of the engrafted islets (color coded).

The application of  $^1\text{H}$  and  $^{19}\text{F}$  MRI to the anterior chamber model resulted in quantitative visualization of PFC labeled implanted islets, hereby providing an independent method for fluorescence methods (see Figure 6.4).

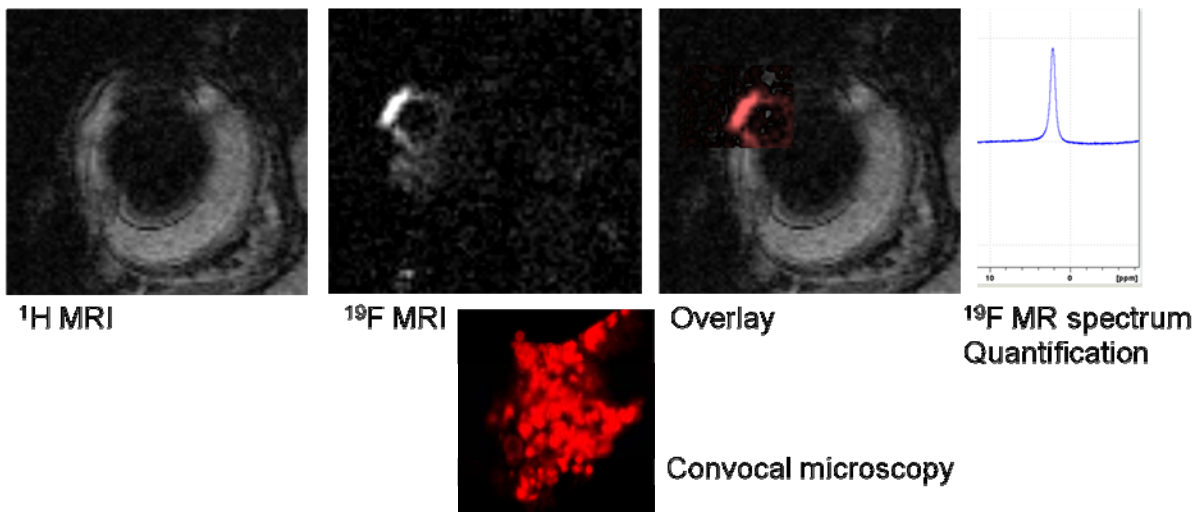


**Figure 6.4:** Top row from left to right: Anatomical image of the eye ( $^1\text{H}$  MRI); visualization of engrafted islets using  $^{19}\text{F}$  MRI; overlay of the  $^1\text{H}$  and  $^{19}\text{F}$  MRI of the anterior chamber model and  $^{19}\text{F}$  NMR spectrum for indirect islet robust quantification. The fluorescent microscopy image below confirms successful labeling of the implanted islets.

### Quantitative *in vivo* imaging using manganese-based MRI contrast

Manganese-based MRI protocols were developed for the visualization of tissue-specific accumulation of  $\text{Mn}^{2+}$  with the aim to visualize the rodent pancreas and the assess its function non-invasively. An optimized protocol of T1-weighted MR imaging of the abdomen fulfilled the requirements of least-invasive MR imaging of tissue specific  $\text{Mn}^{2+}$ -accumulation (see also Figure



6.5). As presented under WP7, this method is sensitive to visualize non-invasively pathological changes during the progression of diabetes.

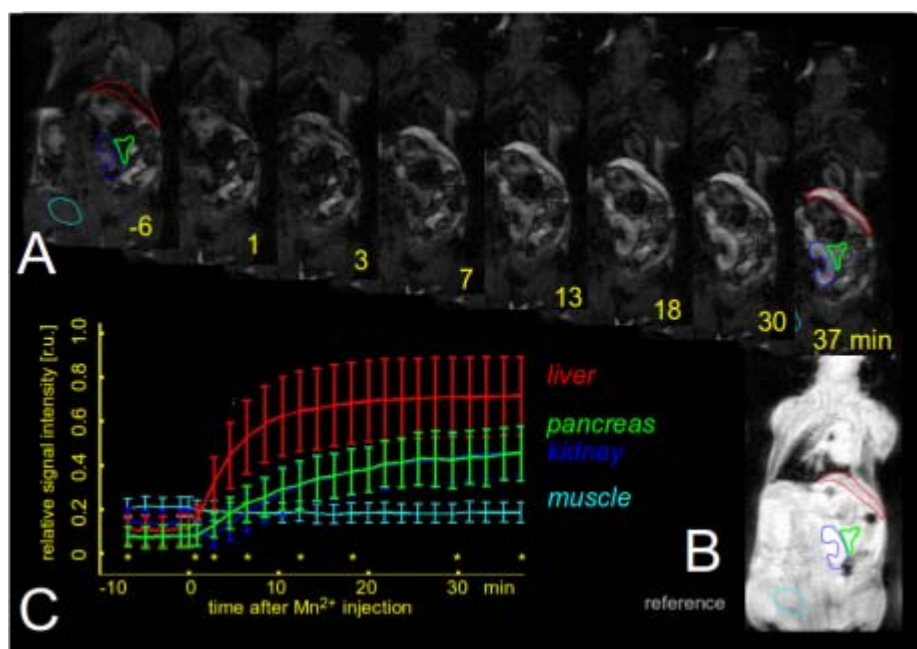


**Figure 6.5: Typical time course experiment after Mn<sup>2+</sup>-injection.**

**A:** Time course of MR images. Numbers indicate time relative to Mn<sup>2+</sup>-injection at t=0min.

**B:** Reference MR-image without inversion preparation.

**C:** Graph of relative signal intensities (reference: "B") in tissue specific ROIs. Error bars represent the scatter of signal intensities in the selected ROIs, not the measurement error! Yellow asterisks indicate times of MR-images in "A".

## WP 7 Therapeutic Applications: *in vitro* and *in vivo* testing

In WP 7 we provided:

- Instrumentation for monitoring of morphological/ biochemical/ pharmacological changes, e.g. a robust method for 3D MR imaging of the mouse abdomen (in collaboration with WP 6)
- A thorough understanding of the molecular drug target for the therapeutic intervention

### **Putative drug candidates for targeted delivery to the $\beta$ -cell**

Specific targeting of the  $\beta$ -cell to improve  $\beta$ -cell survival and function is currently one of the most challenging aims in diabetes therapy. Thus, delivering anti-apoptotic agents directly to the pancreatic islets *via*  $\beta$ -cell specific drug-loaded nanocontainers, as proposed in VIBRANT, is a promising strategy. We have shown that inflammation processes play a pivotal role in diabetes. If islets are exposed, either directly to pro-inflammatory cytokines or are damaged through gluco- and lipotoxicity, cytokine release within the islets leads to  $\beta$ -cell apoptosis and impaired function. According to our studies, three classes of drugs are able to prevent the activation of NF $\kappa$ B, being one of the major pro-apoptotic pathways in the  $\beta$ -cell. Hence, the interleukin-antagonist IL-1Ra, the histone deacetylase inhibitor ITF2357 and c-Jun N-terminal kinase inhibitors restore  $\beta$ -cell function and survival under diabetogenic conditions in animal models *in vivo*, and in human islets *in vitro*<sup>13</sup>. Special polyester block copolymers such as poly(caprolactone-*b*-ethylene glycol) (PCL-PEG) and its copolymers with polyglycolide (PCL/PGL-*b*-PEG) were used for the encapsulation. It was shown that these nanocontainers collapse e.g. upon endosomal acidification and release their payload.

## Robust 3D MR imaging of the mouse abdomen

In order to gain insight about the morphological and functional changes induced by external stimulation, a robust 3D MRI measurement technique, as well as an improved method for the analysis of  $\beta$ -cell function/ mass and measurement techniques of the mouse abdomen were established<sup>14</sup>.  $\beta$ -cell function rather than  $\beta$ -cell mass can be estimated by means of divalent manganese ions ( $Mn^{2+}$ ).  $Mn^{2+}$  (like  $Ca^{2+}$ ) enters metabolically active  $\beta$ -cells through voltage-gated calcium channels, which open in response to a rise in extracellular glucose (Fig.1)<sup>15</sup>. Therefore,  $Mn^{2+}$  uptake is glucose dependent and can be used *in vivo* to assess the functionality of both grafted and endogenous pancreatic islets. MRI signal intensities of paramagnetic  $Mn^{2+}$  and  $\beta$ -cell function were well correlated, as demonstrated in diabetic and non-diabetic mice (Fig.7.2).

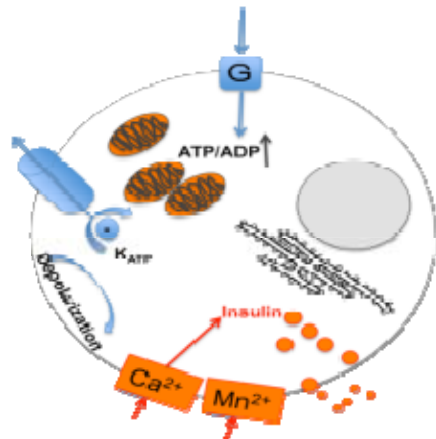


**Fig.7.1:**  $Mn^{2+}$  enters the  $\beta$ -cell in a glucose dependent manner through  $Ca^{2+}$  channels

Representative 3D-MR images of a normal diet fed wild type (WT) C57Bl/6J mouse are shown in Figure 7.2 below. Circles mark our regions of interest in the pancreas.

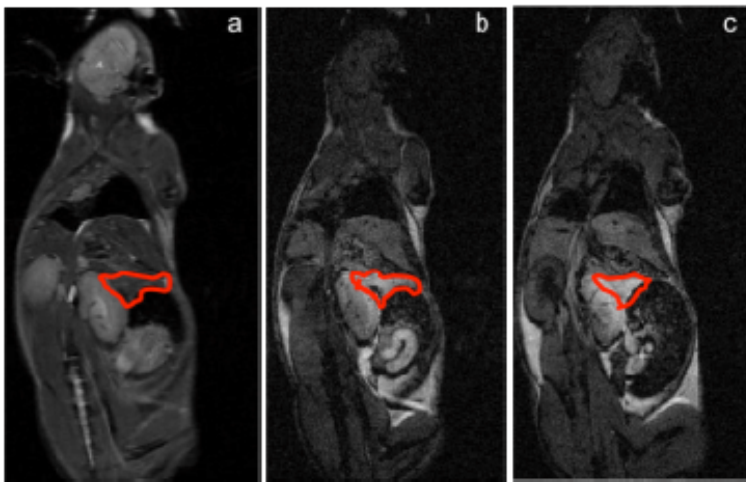


**Fig.7.2:** T1-weighted MR images of whole mouse using the RARE 2D (a) and irFLASH\_2D (b, c) sequence showing the marked pancreas. (b) and (c) are two consecutive sections of the same irFLASH\_2D scan.

### Parameters:

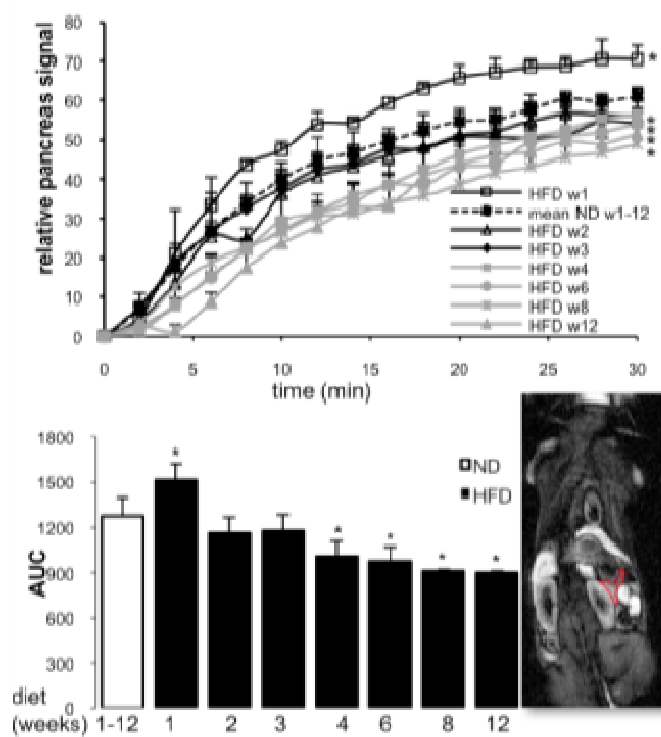
- Animal in prone position
- breathing rate during measurement- 40-50 bpm by manual adjustment
- 72m Quad resonator, zero shims

## No long-term effect of $Mn^{2+}$ on glucose tolerance

To detect the effect of  $Mn^{2+}$  on glucose tolerance,  $MnCl_2$  or vehicle control was injected once weekly in 3 consecutive and ipGTT measured before, immediately after injection and at days 1 and 3. Despite the expected changes in ipGTT after  $MnCl_2$  injection, the effect was not severe and was washed out 2 days after each injection. The results show that also multiple Mn-injections had no long-term effects on glucose tolerance and can therefore be considered as safe tool, which does not affect glucose tolerance.

## Measuring functional $\beta$ -cell mass by non-invasive MRI

To analyze  $\beta$ -cell function and mass during diabetes progression, C57Bl/6 mice were fed a normal chow diet (ND) or a high fat high sucrose diet (HFD, Surwit) and were compared by analyzing *in vivo*-ipGTT, insulin secretion,  $Mn^{2+}$  signals in the MRI and  $\beta$ -cell mass in fixed tissue.



We have shown before<sup>13b)</sup> that the HFD results in impaired glucose tolerance after 4 weeks impaired fasting glucose and hyperinsulinemia after 8 weeks and hyperglycaemia after 12 weeks of diet. Accordingly,  $\beta$ -cells compensate and increase their mass from 4 to 12 weeks of diet, but  $\beta$ -cell mass is decreased after 16 weeks of diet<sup>13i),16</sup> MRI signals showed an initial induction after 1 week of HFD feeding, but from 4 weeks on, there was a decline in MRI signal intensity, which highly correlated with the impaired  $\beta$ -cell function after 4 weeks of HFD feeding (Fig.7.3).

**Fig.7.3:** Relative pancreas signal normalized to liver signal in MRT during 30 min of analysis from age-matched normal diet (ND) and high fat diet (HFD) fed mice over 12 weeks. Each data point represents 3 mice, area under the curve (AUC) was analyzed from the 30 minutes of measurement.

## Progressive impairment of $\beta$ -cell function and mass during 12 weeks of HFD correlates with the MRI signal

After 4 weeks of diet, glucose tolerance and insulin secretion were impaired, but mice compensate by increasing  $\beta$ -cell mass. In line with the impaired function but in contrast to the increased  $\beta$ -cell mass,  $Mn^{2+}$  uptake in the pancreas is lower in the HFD fed mice.

Data from the MRI analysis highly correlate with the functional measures of  $\beta$ -cell function. Finally,  $\beta$ -cell mass was analyzed in the same mice over 12 weeks. Again, the compensatory increase in  $\beta$ -cell mass already after 1-3 weeks correlates with (1) the improved function and (2) the increased MRI signal. In contrast,  $\beta$ -cell mass increases up to 8 weeks of diet, and after 12 weeks, a drop in  $\beta$ -cell mass is observed. Such correlation was confirmed in another mouse model of diabetes.

Our results provide for a 1<sup>st</sup> time a non-invasive measurement of functional  $\beta$ -cell mass during diabetes progression. We further provide here a method to reduce the number of mouse in an experiment, since  $\beta$ -cell mass can be monitored in one mice over a period of time, which highly complies to the 3R (refinement, replacement, reduction) rules of experiments with laboratory animals.

In summary, we achieved:

- **Robust 3D MR imaging** of the mouse abdomen
- Targeting of  $\beta$ -cell survival and function *in vivo*
- Analysis of  $\beta$ -cell function/ mass and measurement techniques of the mouse abdomen with manganese in 2 animal models of diabetes

- Analysis of the first distributed FPNCs delivered by the project partners
  - Treatment of  $\beta$ -cells with functionalized particles *in vitro*
  - Injection, recognition and quantification of **functionalized particles in mice** were accomplished.
- First evidence that drug-loaded NCs specifically support pro-survival in  $\beta$ -cells.

**CONCLUSION:  $Mn^{2+}$ -enhanced MRI can detect small changes in functional  $\beta$ -cells *in vivo* and is a potential method for early noninvasive detection of changes in functional  $\beta$ -cell mass.**

## WP 8: Cross validation

For the development of systemically administered contrast agents intended for non-invasive imaging by MRI (as pursued within VIBRANT) the possibility to cross evaluate the contrast agent up-take specificity throughout the volume of the gland and to calibrate the non-invasive read out is of outmost importance. Optical Projection Tomography (OPT) imaging currently provides the highest resolution available for whole organ *ex vivo* imaging of islets in intact pancreata. In WP 8, this technique has been further improved to generally increase the quality of the generated data and to enable cross-validation studies of MRI imaging of pancreatic islets. Further, the cell-level resolution imaging technique Selective Plane Illumination Microscopy (SPIM) has been integrated into the OPT setup to enable complementary high-resolution cross validation studies. Proof of principle for the successful adaptation/ development of the two technologies for these undertakings has been obtained within WP8. However, the lack of functional nano-containers has impeded their full implementation in the project.

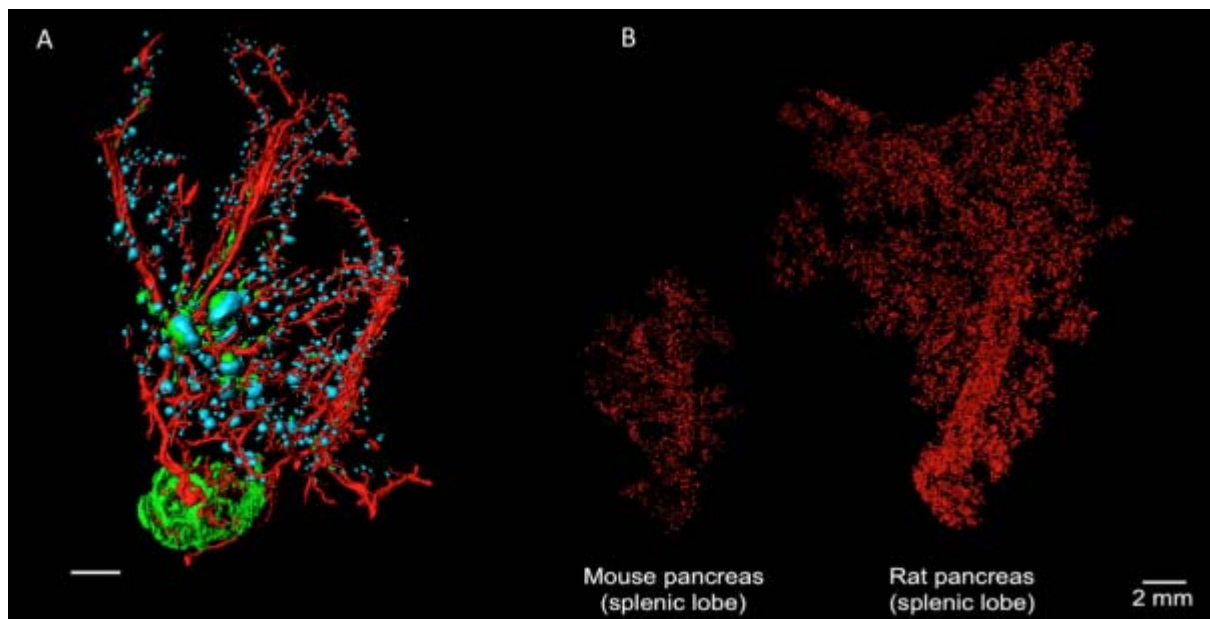


**Fig. 8.1:** Near-infrared OPT images of rodent pancreata **A**, OPT image of a Non Obese Diabetic (NOD) pancreas labeled for ASMA (blood vessels, red, Insulin ( $\beta$ -cells, blue) and CD3 (autoimmune T-cells, green) illustrating the multichannel capacity of the technique. **B**, OPT generated image of a mouse pancreas (left) and a rat pancreas (right). The rat pancreas is around 5 times larger than its mouse counterpart and could not be imaged intact by previous OPT setups. The islets are reconstructed based on the signal from insulin specific antibodies (red).



## Development/optimization of protocols for OPT based cross evaluation.

New image processing assisted algorithms for OPT were developed that generally contribute to increase acquisition speed and quality of pancreatic OPT data. More specifically this included 1) algorithms for semi-automatic and precise positioning of a sample at the axis of rotation, 2) a fast and robust algorithm for determination of post alignment values throughout the specimen as compared to existing methods<sup>17</sup>, and 3) a computational statistical approach implementing the concept of contrast limited adaptive histogram equalisation (CLAHE). The latter approach significantly increases both, the sensitivity of OPT for islet imaging and the conservation of islet morphology<sup>18</sup>. Further, by adapting the OPT technology to enable imaging in the near infrared range the imaging depth and multichannel capacity of the technique could be significantly increased. The latter feature is a pre-requisite for conducting cross-evaluation experiments of MRI contrast agents (having a fluorescent label)<sup>19</sup>. Finally, an approach was developed to improve structural data obtained from Optical Projection Tomography (OPT) using Image Fusion (IF) and contrast normalization. This enables the visualization of molecular expression patterns in biological specimens with highly variable contrast values. As such the technique may e.g. be used to study islet grafts in relation to vascular networks in experimental research.<sup>20</sup>

## Co-registration of OPT and MRI

The capacity for simultaneous detection of fluorochrome labelled MRI contrast agents and antibody labelled islets in “pancreas phantoms” by OPT was evaluated. Hereby islets were labeled *ex vivo* using fluorescent magnetic particles and grafted into excised pancreata to generate the correct anatomical context for imaging assessments. Using such embedded *ex vivo* pancreases, it was

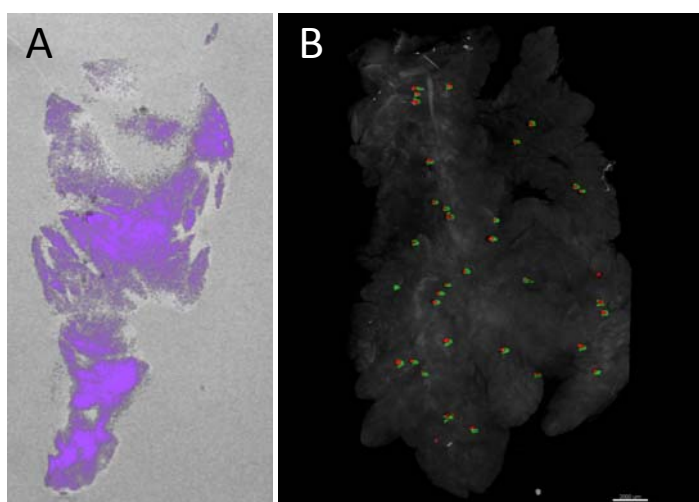


**Fig. 8.2:** 3D Co-registration of OPT and MR images in a pancreas phantom harbouring *ex vivo* labelled islets. Panel A shows the co-registration of the OPT (purple) and the MR image (grey) of a pancreas. In panel B, the signal of prelabeled islets from OPT imaging is shown in red and the MRI signal is shown in green. The tissue outline (in grey) is reconstructed based on tissue autofluorescence using OPT. Artefacts from air bubbles trapped in the agarose have been manually removed. By the implementation of a set of computational techniques the absolute majority of islets detected by OPT can also be recognized by MRI showing that the technique may be used to directly evaluate up-take specificity of *in vivo* labelled islets and for calibration of non-invasive read outs. Note: Endogenous islets are not displayed in the image.

established that islets can be imaged by both methods. A pipeline (software) was developed to co-register OPT and MR images, segment the pancreas and quantify the number of pancreatic islets. As expected, MRI showed some false-positive signals due to intrinsic hypointense contrast. Those results confirmed that OPT is a valuable tool for future cross-validation of *in vivo* MRI of labelled islets. In the process of developing the cross-validation procedure, a range of tissue processing protocols were evaluated and a technique was identified that allows clearing of the sample for OPT and SPIM imaging as well as for MRI using “negative” contrast (manuscript in preparation).

## Integration of SPIM into the OPT setup and high-resolution mesoscopic analyses.

A main objective for WP8 was the proof-of-principle for the utility of the 3D tiling approach. The tiling allows for gathering high resolution data of mesoscopic samples in a whole intact organ like the pancreas. Two mesoscopic imaging techniques (OPT and SPIM) were combined in one single setup. Hereby, to our knowledge, a worldwide unique setup was generated. Imaging with the new setup showed a significant higher resolution and detail in its sub-tiles compared to data that was acquired previously by OPT. Further improvement to the optical coupling of the resonant scan mirror and increased precision of sample positioning in the hybrid imaging setup allowed imaging an entire pancreatic lobe in high resolution with multispectral capabilities.

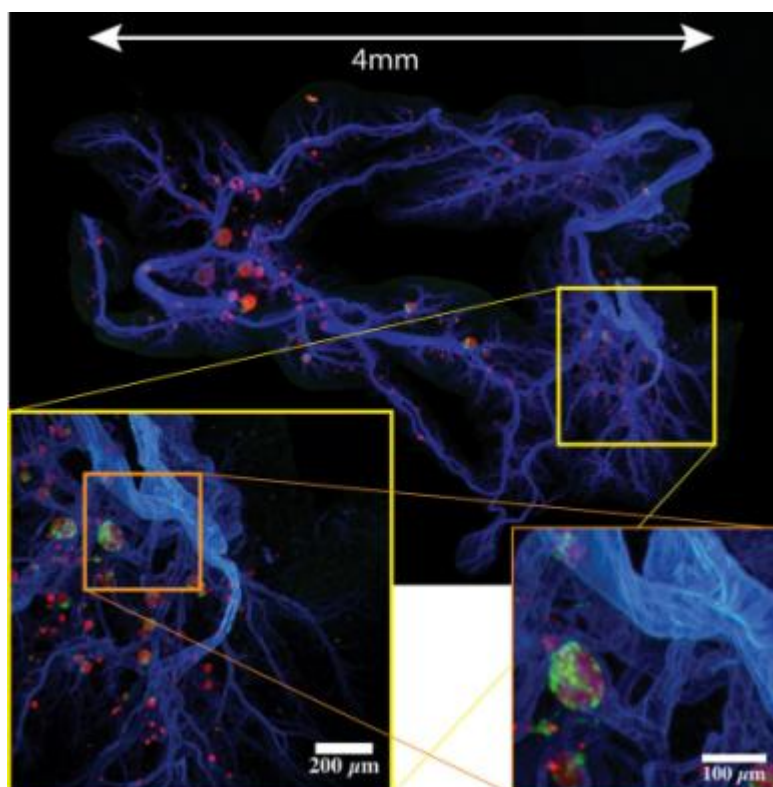


**Fig. 8.3:** SPIM scan of a gastric lobe of murine pancreas, showing a stitched maximum projection. Insets reveal the high resolution achieved. Blood vessels labelled in blue, alpha cells in green and beta-cells in red. The islets of Langerhans show an almost complementary composition of alpha- and beta-cells, as they are the major components in the islets.

## References

- Speier et al., Nature Medicine, 2008, 14, 574 – 578.
- <sup>2</sup> Niehaus JS et al., patent application [WO2009101091 A1](#)
- <sup>3</sup> <http://www.can-hamburg.de/english/menu/products/candots-series-a.html>
- <sup>4</sup> [http://www.strem.com/uploads/web\\_structures/48-1011.gif](http://www.strem.com/uploads/web_structures/48-1011.gif)
- <sup>5</sup> Ran C, et al., Angew. Chem. Int. Ed. 2007, 46, 8998-9001.
- <sup>6</sup> Leclercq-Meyer V, Kadiata MM, Malaisse WJ; Int J Mol Med. 2000,6(2),143-52.
- <sup>7</sup> Ueberberg S et al., Diabetes October 2009, 58 (10), 2324-2334
- <sup>8</sup> a) Poeselt E, Kloust H et al., patent application EP2585210, b) Kloust H et al. Langmuir 2012, 28, 7276-7281, c) *ibid*, 2013, 29 (15), 4915–4921.
- <sup>9</sup> Malaisse WJ, et al. Arch Biochem Biophys. 2012 Jan 15;517(2):138-43
- <sup>10</sup> Thiem J et al., patent application WO2012016935A1.
- <sup>1</sup> Kloust H, et al., J. Phys. Chem. (manuscript submitted)
- <sup>12</sup> Malaisse WJ et al., Met Funct Res Diab, 2013, (Online) Vol 6, 1-5
- <sup>13</sup> a) Lundh M, Christensen DP, Rasmussen DN, Mascagni P, Dinarello CA, et al. Diabetologia (2010) 53, 2569-2578. b) Mandrup-Poulsen T, Pickersgill L, Donath MY; Nat Rev Endocrinol (2010) 6, 158-166. c) Lewis EC, Blaabjerg L, Storling J, Ronn SG, Mascagni P, et al. Mol Med (2011) 17, 369-377. d) Ablamunits V, Henegariu O, Hansen JB, Opare-Addo L, Preston-Hurlburt P, et al. Diabetes (2012) 61, 145-154.

- e) Cavelti-Weder C, Babians-Brunner A, Keller C, Stahel MA, Kurz-Levin M, et al. *Diabetes Care* (2012) 35, 1654-1662. f) Lundh M, Christensen DP, Damgaard Nielsen M, Richardson SJ, Dahllof MS, et al. *Diabetologia* (2012) 55, 2421-2431. g) Maedler K, Dharmadhikari G, Schumann DM, Storling J. *Handb Exp Pharmacol* (2011), 257-278. h) Ardestani A, Sauter NS, Paroni F, Dharmadhikari G, Cho JH, et al. *J Biol Chem*. 2011; 286(19), 17144–17155. i) . Owyang AM, Maedler K, Gross L, Yin J, Esposito L, et al. *Endocrinology*. 2010, 151(6), 2515-27. j) Sauter NS, Schulthess FT, Galasso R, Castellani LW, Maedler K; *Endocrinology* 2008, 149, 2208-2218.
- <sup>14</sup> a) Haase A, Matthaei D, Bartkowski R, Duhmke E, Leibfritz D; *J Comput Assist Tomogr* (1989) 13, 1036-1040. b) Kustermann E, Meyer A, Godbole A, Dreher W, Maedler K; 19th Annual Meeting & Exhibition International Society for Magnetic Resonance in Medicine (2010). c) Kustermann E, Meyer A, Godbole A, Dreher W, Maedler K; *Proc Intl Soc Mag Reson Med* 2011, 19, 810.
- <sup>15</sup> Malaisse WJ, Maedler K; *Diabetes Res Clin Pract*. 2012, 98 (1), 11–18.
- <sup>16</sup> Glas R, Sauter NS, Schulthess FT, Shu L, Oberholzer J, et al. *Diabetologia* 2009, 52, 1579-1588.
- <sup>17</sup> Cheddad et al., *IEEE Transactions on medical imaging*, 2012
- <sup>18</sup> Hörnblad A, Cheddad A, Ahlgren U; *Islets* 2011, 3, 204–208

## 4. Use and dissemination of foreground

A plan for use and dissemination of foreground (including socio-economic impact and target groups for the results of the research) shall be established at the end of the project. It should, where appropriate, be an update of the initial plan in Annex I for use and dissemination of foreground and be consistent with the report on societal implications on the use and dissemination of foreground (section 4.3 – H).

The plan should consist of:

- Section A

This section should describe the dissemination measures, including any scientific publications relating to foreground. **Its content will be made available in the public domain** thus demonstrating the added-value and positive impact of the project on the European Union.

- Section B

This section should specify the exploitable foreground and provide the plans for exploitation. All these data can be public or confidential; the report must clearly mark non-publishable (confidential) parts that will be treated as such by the Commission. Information under Section B that is not marked as confidential **will be made available in the public domain** thus demonstrating the added-value and positive impact of the project on the European Union.



## Section A (public)

This section includes two templates

- Template A1: List of all scientific (peer reviewed) publications relating to the foreground of the project.
- Template A2: List of all dissemination activities (publications, conferences, workshops, web sites/applications, press releases, flyers, articles published in the popular press, videos, media briefings, presentations, exhibitions, thesis, interviews, films, TV clips, posters).

These tables are cumulative, which means that they should always show all publications and activities from the beginning until after the end of the project. Updates are possible at any time.

TEMPLATE A1: LIST OF SCIENTIFIC (PEER REVIEWED) PUBLICATIONS, STARTING WITH THE MOST RECENT										
NO.	Title	Main author	Title of the periodical or the series	Number, date or frequency	Publisher	Place of Publication	Year of Publication	Relevant pages	Document Identifier	Is/Will open access[2] provided to this publication ?
1	In situ labeling and imaging of endogenous neural stem proliferation and migration.	G. Vande Velde, S. Couillard-Despres, L. Aigner, U. Himmelreich and A. Van der Linden	WIREs Nanomedicine and Nanobiotechnology	4			2012	663-679		no
2	D-Gluc-hept-2-ulose and Novel Deoxyfluoro Derivatives as Seven-Carbon Analogues of F-Deoxy-d-glucose (FDG)	Yevgeniy Leshch, Daniel Waschke, Julian Thimm, Joachim Thiem	Synthesis	23	Thieme	Germany	2011	3871-3877	DOI: 10.1055/s-0031-1289598	no
3	Microwave-Assisted Synthesis of Triazole-Linked Phthalocyanine-Peptide Conjugates as Potential Photosensitizers for Photodynamic Therapy	Nadezhda V. Sokolova, Theo Schotten, Herwig J. Berthold, Joachim Thiem, Valentine G. Nenajdenko	Synthesis	45	Thieme	Germany	2013	556-561		no

4	Biomedical molecular imaging	U. Himmelreich	Publ. Serv. Rev.: Euro. Sci. Technol.	16	Publ. Serv. Rev.	London, UK	2012	212-213		No
5	Investigating the Pancreatic Function: Robust 3D MR imaging of Mouse Abdomen	Kustermann E, Meyer A, Godbole A, Dreher W, Maedler K	Proc. Intl. Soc. Mag. Reson. Med.	19			2011	810		no
6	Noninvasive in vivo model demonstrating the effects of autonomic innervation on pancreatic islet function.	Rodriguez-Diaz R, et al.	Proc Natl Acad Sci USA	No 109	PNAS	USA	2013	pp. 21456-61		no
7	Glucagon regulates its own synthesis by autocrine signaling.	Leibiger B, et al.	Proc Natl Acad Sci USA	No 109	PNAS	USA	2013	pp. 20925-30		no
8	Inositol hexakisphosphate suppresses excitatory neurotransmission via synaptotagmin-1 C2B domain in the hippocampal neuron.	Yang SN, et al.	Proc Natl Acad Sci USA	No 109	PNAS	USA	2012	pp. 12183-88		no
9	High-resolution, noninvasive longitudinal live imaging of immune responses.	Abdulreda MH, et al.	Proc Natl Acad Sci USA	No 108	PNAS	USA	2011	pp. 12863-68		no
10	Lowering apolipoprotein CIII delays onset of type 1 diabetes.	Holmberg R, et al.	Proc Natl Acad Sci USA	No 108	PNAS	USA	2011	pp. 10685-89		no
11	Quantification of lung fibrosis and emphysema in mice using automated micro-computed tomography.	E. De Langhe, G. Vande Velde, J. Hostens, U. Himmelreich, B. Nemery, F.P. Luyten, J. Vanoirbeek and R.J. Lories	PLoS ONE	7(8)			2012	e43123 (1-11)		yes
12	Highly Efficient Synthesis of Ketoheptoses	. Waschke, J. Thimm, J. Thiem	Org. Lett.	13	American chemical Society (ACS)	USA	2011	3628-3631		no

13	Improving signal detection in emission optical projection tomography via single source multi-exposure image fusion	Cheddad A, Nord C, Hörnblad A, Prunskaitė-Hyyryläinen R, Eriksson M, Georgsson F, Vainio SJ, Ahlgren U	Opt Express	Jul 15;21(14)			2013	16584-604	-	No
14	Magnetic resonance-based cell imaging using contrast media and reporter genes.	G. Vande Velde and U. Himmelreich	New applications of NMR in drug discovery and development.		Royal Society of Chemistry (RSC)	Cambridge, Untited Kingdom	2013	293-329		no
15	Amphiphilic, cross-linkable diblock copolymers for multifunctionalized nanoparticles as biological probes	Christian Schmidtke, Elmar Pösel, Johannes Ostermann, Andrea Pietsch, Hauke Kloust, Huong Tran, Theo Schotten, Neus G. Bastús, Robin Eggers Horst Weller	Nanoscale	5	Royal Society of Chemistry (RSC)	Cambridge, Untited Kingdom	2013	7433-7444		No
16	Magnetic layer-by-layer coated particles for efficient magnetic resonance imaging of dendritic cells and mesenchymal stem cells.	M.-L. De Temmerman, S.J. Soenen, N. Symens, B. Lucas, R.E. Vandenbroucke, C. Libert, J. Demeester, S.C. De Smedt, U. Himmelreich and J. Rejman	Nanomed.	in press	Elsevier	USA	2013			no
17	Immunocytochemistry of GLUT2, uptake of fluorescent desnitro-streptozotocin analogs and phosphorylation of D-glucose in INS-1E cells	M. Virreira, J. Popescu, C. Gillet, Y. Zhang, Y. Leshch, J. Thimm, J. Thiem, W. J. Malaisse, A. Sener	Mol. Med. Rep.	8			2013	473-479		no
18	Effects of distinct nanoparticle preparations upon insulin release and glucose metabolism in incubated rat pancreatic islets.	Sener, Y. Zhang, K. Werner, J. S. Niehaus, T.Schotten, W. J. Malaisse	Metab. Funct. Res. Diab.	6			2013	pp. 1-5		no
19	Insulin release from isolated pancreatic islets, dispersed islet cells and tumoral insulin producing cells: a re-examination	N. Bulur, Y. Zhang, W.J. Malaisse, A. Sener	Metab. Funct. Res. Diab	3			2010	20-24		no

20	In Situ Functionalization and PEO Coating of Iron Oxide Nanocrystals Using Seeded Emulsion Polymerization	Hauke Kloust, Christian Schmidtke, Artur Feld, Theo Schotten, Robin Eggers, Ursula E. A. Fittschen, Florian Schulz, Elmar Pösel, Johannes Ostermann, Neus G. Bastús, Horst Weller	Langmuir	29	American chemical Society (ACS)	USA	2013	4915–4921		No
21	Ultrasmall Biocompatible Nanocomposites: A New Approach Using Seeded Emulsion Polymerization for the Encapsulation of Nanocrystals	Hauke Kloust, Elmar Pösel, Sascha Kappen, Christian Schmidtke, Andreas Kornowski, Werner Pauer, Hans-Ulrich Moritz, Horst Weller	Langmuir	28	American chemical Society (ACS)	USA	2012	7276–7281		No
22	Covalent attachment of polymersomes to surfaces	S. Domes, V. Filiz, J. Nitsche, A. Frömsdorf, S. Förster	Langmuir	26(10)	American chemical Society (ACS)	USA	2010	6927–6931		no
23	Radical Initiated Reactions on Biocompatible CdSe-Based Quantum Dots: Ligand Cross-Linking, Crystal Annealing, and Fluorescence Enhancement	Christian Schmidtke, Holger Lange, Huong Tran, Johannes Ostermann, Hauke Kloust, Neus G. Bastús, Jan-Philip Merkl, Christian Thomsen, Horst Weller	J. Phys. Chem. C	117	American chemical Society (ACS)	USA	2013	8570–8578		no
24	Design and evaluation of theranostic perfluorocarbon particles for simultaneous antigen-loading and 19F-MRI tracking of dendritic cells.	H. Dewitte, B. Geers, S. Liang, U. Himmelreich, J. Demeester, S.C. De Smedt and I. Lentacker	J. Control. Release	169	Elsevier	USA	2013	141-149		no
25	Transplantation into the anterior chamber of the eye for longitudinal, non-invasive in vivo imaging with single-cell resolution in real-time.	Abdulreda MH, et al.	J Vis Exp	No 73	MyJoVE Corp.	USA	2013	e50466		yes
26	Near infrared optical projection tomography for assessments of b-cell mass distribution in diabetes research.	A.U.Eriksson, C. Svensson, A. Hörnblad, A. Cheddad, E.Kostromina, M. Eriksson, N. Norlin, A. Pileggi, J. Sharpe, F. Georgsson, T. Alanentalo, U. Ahlgren	J Vis Exp	Jan; 12 (71)	MyJoVE Corp.	USA	2013		<a href="http://dx.doi.org/10.3791/50238">http://dx.doi.org/10.3791/50238</a>	yes

27	An improved protocol for optical projection tomography imaging reveals lobular heterogeneities in pancreatic islet and $\beta$ -cell mass distribution	Hörnblad, A. Cheddad and U. Ahlgren	Islets	3(4)	Landes bioscience		2011	204-8	<a href="http://www.ncbi.nlm.nih.gov/pmc/articles/PMC2163319/">http://www.ncbi.nlm.nih.gov/pmc/articles/PMC2163319/</a>	Yes
28	One-step purification of functional human and rat pancreatic alpha cells.	Köhler M, et al.	Integrative Biology	No 4			2012	pp. 209-19		no
29	Exploring the pancreas with optical projection tomography (Editorial)	Ulf Ahlgren	Imaging Med	Feb 2012, Vol. 4, No. 1	Future medicine		2012	41460		no
30	Image Processing Assisted Algorithms for Optical Projection Tomography.	Cheddad A, Svensson C, Sharpe J, Georgsson F, Ahlgren U.	IEEE, Trans. Med. Imaging	31(1)	IEEE Magnetics Society	USA	2012	1-15	<a href="http://dx.doi.org/10.1109/TMI.2011.2161590">http://dx.doi.org/10.1109/TMI.2011.2161590</a>	no
31	Synthesis of PEGylated Magnetic Nanoparticles with Different Core Sizes.	J. Trekker, K. Jans, H. Damm, D. Mertens, T. Nuytten, J. Vanacken, V. Moshchalkov, J. d'Haen, T. Stakenborg, W. Van Roy, U. Himmelreich and L. Lagae	IEEE Trans. Magn.	49	IEEE Magnetics Society	USA	2013	219-226		no
32	Synthesis of fluorinated ketoheptoses as specific diagnostic agents.	D. Waschke, Y. Leshch, J. Thimm, U. Himmelreich and J. Thiem	Eur. J. Org. Chem.	2012(5)	Wiley	Germany	2012	948-959		no
33	Imaging Dynamics of CD11c+ Cells and Foxp3+ Cells in Progressive Autoimmune Insulinitis	Anja Schmidt-Christensen, Lisbeth Hansen, Erwin Ilegems, Shashank Gupta, Ulf Dahl, Åsa Larefalk, Nina Fransén-Pettersson, Tine D. Hannibal, Alexander Schulz, Per-Olof Berggren, and Dan Holmberg.	Diabetologia	in press			2013			no
34	Imaging of the b-cells of the islets of Langerhans	Willy J. Malaisse Kathrin Maedler	Diabetes Research and Clinical Practice	98	Elsevier		2012	pp. 11-18		no

35	Donor islet endothelial cells in pancreatic islet revascularization.	Nyqvist D, et al.	Diabetes	No 60			2011	pp. 2571-77		No
36	In vivo monitoring of cell based therapy in the liver.	A. Ketkar-Atre and U. Himmelreich	Curr. Mol. Imag.	2	Bentham Science	USA	2013	164-176		no
37	Evaluation of manganese uptake and toxicity in mouse brain during continuous MnCl <sub>2</sub> administration using osmotic pumps.	M.R. Sepúlveda, T.Dresselaers, P.Vangheluwe, W. Everaerts, U.Himmelreich, A.M. Mata and F. Wuytack	Contrast Media Mol. Imag	7			2012	426-434		yes
38	Expression and localization of glucose transporters in rodent submandibular salivary glands	S Cetik, W. J. Malaisse, A. Sener, I. Ristea Popescu	Cell. Physiol. Biochem.	submitted						no
39	Ultrastructural analysis and magnetic resonance imaging of human dental pulp stem cells in vitro and in vivo.	T. Struys, P. Gervois, A. Ketkar-Atre, C. Leten, W. Martens, A. Bronckaers, T. Dresselaers, C. Politis, I. Lambrichts and U. Himmelreich	Cell Transplantation	in press	Cognizant Communication Publications	USA	2013			yes
40	Apolipoprotein CIII hyperactivates $\beta$ cell Cav1 channels through SR-BI/ $\beta$ 1 integrin-dependent coactivation of PKA and Src.	Y Shi, G Yang, J Yu, L Yu, R Westenbroek, WA Catterall, L Juntti-Berggren, P-O Berggren & S-N Yang	Cell Mol Life Sci	in press	Springer	Germany	2013		doi: 10.1007/s00018-013-1442-x	no
41	Transthyretin binds to glucose-regulated proteins and is subjected to endocytosis by the pancreatic $\beta$ -cell.	Dekki N, et al.	Cell Mol Life Sci	No 69	Springer	Germany	2012	pp. 1733-43		no
42	Innervation patterns of autonomic axons in the human endocrine pancreas.	Rodriguez-Diaz R, et al.	Cell Metab	No 14			2011	pp. 45-54		no
43	MRI assessment of blood outgrowth endothelial cell homing using cationic magnetoliposomes.	S.J. Soenen, S.F. De Meyer, T.Dresselaers, G. Vande Velde, I.M. Pareyn, K. Braeckmans, M. De Cuyper, U.Himmelreich and K.I. Vanhoorelbeke	Biomaterials	32			2011	4140-4150		no

44	19F-heptuloses as tools for the non-invasive imaging of GLUT2-expressing cells.	W.J. Malaisse, Y. Zhang, K. Louchami, S. Sharma, T. Dresselaers, U. Himmelreich, G.W. Novotny, T. Mandrup-Poulsen, D. Waschke, Y. Leshch, J. Thimm, J. Thiem and A. Sener	Arch. Biochem. Biophys.	517			2012	138-143		no
45	The pancreatic beta cell as a paradigm for advances in inositide research	Barker CJ, Berggren PO	Advances in Biological Regulation	52			2012	361-368		no
46	The pancreatic islet as a signaling hub.	Barker CJ, et al.	Adv Biol Regul	No 53	Elsevier	USA	2013	pp. 156-63		no
47	Non-invasive in vivo imaging of pancreatic $\beta$ -cell function and survival - a perspective.	Leibiger IB, et al.	Acta Physiol (Oxf)	No 204			2012	pp. 178-85		no
48	Tailor-Made Quantum Dot and Iron Oxide Based Contrast Agents for in Vitro and in Vivo Tumor Imaging	Elmar Pösel, Christian Schmidtke, Steffen Fischer, Kersten Peldschus, Johannes Salamon, Hauke Kloust, Huong Tran, Andrea Pietsch, Markus Heine, Gerhard Adam, Udo Schumacher, Christoph Wagener, Stephan Förster, Horst Weller	ACS Nano	6	American chemical Society (ACS)	USA	2012	3346–3355		no
49	Relaxivity Optimization of a PEGylated Iron-Oxide-Based Negative Magnetic Resonance Contrast Agent for T2-Weighted Spin–Echo Imaging	Elmar Pösel, Hauke Kloust, Ulrich Tromsdorf, Marcus Janschel, Christoph Hahn, Christoph Maßlo, Horst Weller	ACS Nano	6	American chemical Society (ACS)	USA	2012	1619–1624		no

50	D-mannoheptulose analogs: tools for non-invasive B-cell imaging?	W.J. Malaisse	Metab Funct Res on Diab (Online)	4	MEFRED		2011	21		Yes
51	Multi-modal imaging of the pancreas and pancreatic islets in rodent models - from ex vivo to in vivo.	U. Himmelreich, A. Atre, A. Eriksson, K. Louchami, D. Waschke, S. Sharma, Y. Zhang, E. Küstermann, J. Thiem, K. Mädler, A. Sener, J. Thimm, W.J. Malaisse, U. Ahlgren.	Metab Funct Res on Diab (Online)	4	MEFRED		2011	16		yes
52	L-glutamate decarboxylase activity in Wistar rats brain and pancreatic islets	A. Rzajeva, K. Louchami, M. Aswendt, U. Himmelreich, A. Sener	Metab Funct Res on Diab (Online)	6	MEFRED		2013	25		yes
53	<sup>19</sup> F-mannoheptuloses as contrast agents for the non-invasive imaging of GLUT2-expressing cells: in vivo and ex vivo MRI studies – latest update.	S. Liang, K. Louchami, H. Kolster, E. Hupkens, W. J. Malaisse, J. Thimm, A. Sener, U. Himmelreich	Metab Funct Res on Diab (Online)	6	MEFRED		2013	16		yes
54	Species-specific differences in islet expression pattern of glucose transporters	R. Popescu, P. Demetter, P. Loi, W.J. Malaisse and A. Sener	Metab Funct Res on Diab (Online)	6	MEFRED		2013	24		yes
55	<sup>19</sup> F-heptuloses as tools for the non-invasive imaging of GLUT2-expressing cells	Y. Zhang	Metab Funct Res on Diab (Online)	6	MEFRED		2013	29		yes
56	<sup>19</sup> F-mannoheptuloses as tools for the non-invasive imaging of GLUT2-expressing cells: ex vivo and in vivo studies	K. Louchami, S. Liang, E. Hupkens, W. J. Malaisse, J. Thimm, A. Sener, U. Himmelreich	Diabetologia	in press			2013			no



TEMPLATE A2: LIST OF DISSEMINATION ACTIVITIES

N O.	Type of activities[1]	Main leader	Title	Date/Period	Place	Type of audience[2]	Size of audience	Countries addressed
1	Conference	A. Ketkar-Atre, K. Louchami, T. Yin, M. De Cuyper, W.J. Malaisse, U. Himmelreich	World Molecular Imaging Society Congress-Savannah: Magnetoliposome for longitudinal follow up of pancreatic islet by MRI	18.09.2013	Georgia, USA	Scientists, Industry		all
2	Conference	Jacobsen A	17th European Carbohydrate Symposium (EUROCARB)	01.07.2013	Tel Aviv, Israel	Scientists, Industry	1000	all
3	Conference, Exhibition	Frank Schröder-Oeynhausen	EuroNanoForum 2013	17.06.2013	Dublin, Ireland	Scientists, Industry	1800	all
4	Conference	Ahlgren U	The 6th workshop on Visualisation of Cells and Tissues by Light Microscopic Techniques and Tomographic Methods	12.06.2013	Oulu, Finland	Scientists	100	all
5	Conference	Berggren PO	4th International Brussels Pancreatic Islet Symposium	30.05.2013	Brussels, Belgium	Scientists, Industry	700	all
6	Exhibition	Jan Niehaus	NSTI 2013	12.05.2013	Washington D.C, USA	Scientists, Industry		
7	Workshop	Maedler K	5th NIH/Juvenile Diabetes Research Foundation (JDRF) workshop on Targeting the Beta Cell for Therapeutics & Imaging	015.04.2013	Bethesda, Maryland, USA	Scientists, Community, Industry, Clinicians	600	all
8	Conference	A. Ketkar-Atre, K. Louchami, U.Himmelreich	Longitudinal follow up of pancreatic islets by MRI using labeling with magnetoliposomes.	01.04.2013	Salt Lake City, USA	Scientists, Community, Industry, Clinicians	5000	all
9	Conference	S. Liang, U.Himmelreich	In vitro and in vivo 19-fluorine magnetic resonance imaging (MRI) of beta-cells and pancreatic using GLUT-2 specific contrast agents.	01.04.2013	Salt Lake City, USA	Scientists, Community Industry, Clinicians	5000	all
10	Conference	Berggren PO	XIV SERVIER-IGIS Symposium	21.03.2013	Saint-Jean-Cap-Ferrat, France	Scientists, Community Industry, Clinicians	150	all
11	Workshop	Berggren PO	UK-Singapore Workshop on Stratified Medicine in Diabetes	25.02.2013	Singapore	Scientists, Clinicians	120	all

12	Interview	Ahlgren U	Swedish Public Radio: <a href="http://sverigesradio.se/sida/artikel.aspx?programid=406&amp;artikel=5427118">http://sverigesradio.se/sida/artikel.aspx?programid=406&amp;artikel=5427118</a>	30.01.2013		General Public		all
13	Conference	Berggren PO	Imaging Symposium	14.01.2013	Copenhagen, Denmark	Scientists, Industry	150	all
14	Conference	Ahlgren U	NovoNordisk Joint BRU and DRU symposium on imaging	14.01.2013	Copenhagen, Denmark	Scientists, Industry	100	all
15	Invited Talk	Ahlgren U	The Royal Belgian Academy of Medicine	15.12.2012	Brussels, Belgium	Scientists	100	all
16	Conference	Berggren PO	1st Annual Meeting, LOEWE-Research Focus Non-Neuronal Cholinergic Systems	10.11.2012	Giessen, Germany	Scientists, Industry,	150	all
17	Conference	Berggren PO	The 2nd POSTECH International Symposium on Bio-Imaging	01.11.2012		Scientists, Industry, Clinicians	1100	all
18	Conference	U.Himmelreich	Labeling with contrast agents – pitfalls and challenges.	01.11.2012	Cologne, Germany	Scientists, Community Industry, Clinicians	50	all
19	Conference	A. Ketkar-Atre, K. Louchami, U.Himmelreich	Non-invasive iron quantification of magnetically labeled cells using electron paramagnetic resonance.	October 2012	Lisbon, Portugal	Scientists, Community Industry, Clinicians	1500	all
20	Exhibition	Jan Niehaus	RUSNANO 2012	30.10.2012	Moscow, Russia	Scientists, Industry,	2000	all
21	Conference	Berggren PO	53rd International Symposium on "Biological Regulation and Enzyme Activity in Normal and Neoplastic Tissue"	17.09.2012	Bologna, Italy	Scientists, Industry, Clinicians	800	all
22	Conference	J. Thimm, W. Malaisse, U.Himmelreich	<sup>19</sup> F-MRI based detection of beta cells using fluoromannoheptuloses.	01.09.2012	Dublin, Ireland	Scientists, Community Industry, Clinicians	2500	all
23	Conference	J. Trekker, U.Himmelreich	Non-invasive quantification of cells using magnetic particles and electron paramagnetic resonance.	01.09.2012	Dublin, Ireland	Scientists, Community Industry, Clinicians	2500	all

24	Conference	A. Ketkar-Atre, U.Himmelreich	Targeted magnetoliposomes for liver imaging.	01.09.2012	Dublin, Ireland	Scientists, Community Industry, Clinicians	2500	all
25	Conference	A. Ketkar-Atre, K. Louchami, U.Himmelreich	Longitudinal MR imaging of pancreatic islets using magnetoliposomes.	01.09.2012	Dublin, Ireland	Scientists, Community Industry, Clinicians	2500	all
26	Conference	Himmelreich U	EASD: Non-invasive in-vivo analysis of $\beta$ -cell function and mass by MRI	01.09.2012	Berlin, Germany	Scientists, Community Industry, Clinicians	1000	all
27	Conference	Leshch Y	26th International Carbohydrate Symposium (ICS 2012)	22.07.2012	Madrid, Spain	Scientists, Industry	1000	all
28	Conference	Jan Niehaus	NSTI 2012	18.06.2012	Santa Clara, California, USA	Scientists, Industry, Clinicians	2000	all
29	Invited Talk	Berggren PO	2012 Kroc Lecture	30.05.2012	Boston, USA	Scientists, Industry, Clinicians	600	all
30	Conference	Berggren PO	Obesity and Diabetes	23.05.2012	Århus, Denmark	Scientists, Community Industry, Clinicians	700	all
31	Conference	U.Himmelreich	Toxicity of nanoparticles.	May 2012	Melbourne, Australia	Scientists, Community Industry, Clinicians	4500	all
32	Conference	J. Trekker, U.Himmelreich	The effect of intracellular clustering on the stability and contrast generating properties of SPIOs: A comparison between PEGylated SPIOs and liposome SPIOs.	May 2012	Melbourne, Australia	Scientists, Community Industry, Clinicians	4500	all
33	Conference	A. Ketkar-Atre, U.Himmelreich	Functionalized magnetoliposomes for visualization of hepatocytes in vitro and in vivo.	May 2012	Melbourne, Australia	Scientists, Community Industry, Clinicians	4500	all

34	Conference	J. Trekker, L. Lagae, U.Himmelreich	Synthesis of iron oxide superparamagnetic nanoparticles with different sizes and their functionalization with a poly-ethylene-glycolated silane.	May 2012	Minneapolis, USA	Scientists, Community Industry, Clinicians	1000	all
35	Conference	J. Trekker, L. Lagae, U.Himmelreich	Optimizing superparamagnetic nanoparticles towards contrast enhanced MRI for sensitive in vivo cell detection.	May 2012	Minneapolis, USA	Scientists, Community Industry, Clinicians	1000	all
36	Conference	Jan Niehaus	BioNanoMed 2012	01.03.2012	Krems, Austria	Scientists, Industry, Clinicians	500	all
37	Conference	Berggren PO	Symposium on "Nanoengineering in Medicine	28.02.2012	Singapore	Scientists, Industry, Clinicians	700	all
38	Workshop	Berggren PO	KAST-KI Workshop – Stem Cell and Diabetics Research Workshop	27.02.2012	Seoul, South Korea	Scientists, Industry, Clinicians	250	all
39	Conference	Berggren PO	The Oxford Centre for Diabetes, Endocrinology & Metabolism (OCDEM) Seminar Series	01.02.2012	Oxford, England	Scientists, Industry, Clinicians	150	all
40	Conference	Theo Schotten	NMP cluster "Targeted Nano-Pharmaceuticals and early Diagnostics" meeting	13.12.2011	Paris, France	Scientists EU project officers	30	EU
41	Conference	Berggren PO	The 10th islet transplantation and beta cell research symposium	26.11.2011	Seoul, South Korea	Scientists, Industry, Clinicians	700	all
42	Conference	Y. Zhang, K. Louchami, S. Sharma, U. Himmelreich, Thimm, W.J. Malaisse, A. Sener	15th Annual Meeting of Chinese Diabetes Society: Inhibition of insulin release by 19F-heptuloses and their uptake by rat hepatocytes	23.11.2011	Beijing, China	Scientists, Industry		all
43	Conference	Berggren PO	SHARE Symposium	16.11.2011	Copenhagen, Denmark	Scientists, Industry	300	all
44	Workshop	Himmelreich U	Juvenile Diabetes Research Foundation (JDRF) workshop on Targeting the Beta Cell for Therapeutics & Imaging Workshop	02.11.2011	New York, USA	Scientists, Industry	200	all
45	Exhibition	Jan Niehaus	BioNanoMed 2010	02.11.2011	Krems, Austria	Scientists, Industry		
46	Exhibition	Frank Schröder-Oeynhausen	RUSNANO 2011	24.10.2011	Moscow, Russia	Scientists, Industry		
47	Conference	Berggren PO	The Annual Pharmaceutical Science Symposium	21.10.2011	Sao Paulo, Brazil	Scientists, Industry	500	all

48	Conference	Schotten T	6 <sup>th</sup> Hanseatic India Colloquium: "New Medicine in a Changing World" Invited Talk, Broadcast Interview	20.10.2011	Hamburg, Germany	Scientists, Industry	200	all
49	Conference	A. Ketkar-Atre, U.Himmelreich	Functionalized magnetoliposomes for hepatocytes' visualization in vitro and in vivo.	October 2011	Leipzig, Germany	Scientists, Community Industry, Clinicians	1000	all
50	Conference	J. Trekker, U.Himmelreich	Intracellular aggregation of nanoparticles increases in vivo cell detectability by MRI.	October 2011	Leipzig, Germany	Scientists, Community Industry, Clinicians	1000	all
51	Conference	Werner K	1 <sup>st</sup> European Congress of Applied Biotechnology	25.09.2011	Berlin, Germany	Scientists, Industry	750	all
52	Workshop	Katja Werner	Nanoparticles for Therapy and Diagnosis of Alzheimer Disease NAD	20.09.2011	Milan, Italy	Scientists		
53	Conference	Theo Schotten	International Conference on Nanosciences & Nanotechnologies Invited Round Table	12.07.2011	Thessaloniki, Greece	Scientists General public Industry	2000	all
54	Conference	Thiem J	16 <sup>th</sup> EuroCarb	03.07.2011	Sorrento, Naples, Italy	Scientists, Industry	1000	all
55	Conference	S.J.H. Soenen, S. De Smedt, U.Himmelreich	Intracellular Nanoparticle Degradation Affects Cell Functionality and Nanoparticle Diagnostics Ability.	July 2011	Singapore, Singapore	Scientists, Community Industry, Clinicians	1500	all
56	Conference	Malaisse WJ, Sener A, Werner K, Niehaus JS,	3 <sup>rd</sup> International Brussels Pancreatic Islet Symposium	30.06.2011	Brussels, Belgium	Scientists, Industry	1000	all
57	Conference	Berggren PO	ADA 71st Scientific Sessions	24.06.2011	San Diego, USA	Scientists, Industry	1000	all
58	Conference	Theo Schotten	MedChem Conference ZHAW: Invited Talk: "VIBRANT a European Project for Betacell Imaging and Quantification"	15.06.2011	Zürich, Switzerland	Scientists Industry	200	all
59	Exhibition	Frank Schröder-Oeynhausen	NSTI 2011	13.06.2011	Boston, Massachusetts USA	Scientists, Community Industry, Clinicians		
60	Conference	U.Himmelreich	Conceptual challenges of in vivo MRI for cell tracking.	June 2011	Leiden, The Netherlands	Scientists, Community, Industry, Clinicians	2000	all

61	Conference	A. Ketkar-Atre, U.Himmelreich	Targeted magnetoliposomes for visualization of hepatocytes.	June 2011	Leiden, The Netherlands	Scientists, Community Industry, Clinicians	2000	all
62	Conference	K. Louchami, E. Küstermann, J. Thiem, K. Mädler, A. Sener, W.J. Malaisse, U. Ahlgren, U.Himmelreich	Multi-modal imaging of pancreas and pancreatic islets in rodent models – from ex vivo to in vivo.	June 2011	Brussels, Belgium	Scientists, Community Industry, Clinicians	300	all
63	Conference, Exhibition	Theo Schotten	EuroNano Forum	30.05.2011	Budapest, Hungary	Scientists Industry	2000	all
64	Conference	Jan Niehaus	Meeting Biomagnetic Particles	11.05.2011	Charleston, South Carolina, USA	Scientists Industry		
65	Conference	Uwe Himmelreich	19 <sup>th</sup> Annual Meeting of the International Society of Magnetic Resonance in Medicine	07.05.2011	Montreal, Canada	Scientists, Industry	1000	all
66	Conference	A. Ketkar-Atre, U.Himmelreich	Targeted magnetoliposomes for visualization of hepatocytes.	May 2011	Montreal, Canada	Scientists, Community Industry, Clinicians	5000	all
67	Conference	S.J.H. Soenen, M. DeCuyper, U.Himmelreich	Magnetoliposomes open up new horizons as MRI contrast agents.	May 2011	Montreal, Canada	Scientists, Community Industry, Clinicians	5000	all
68	Conference	G. Vande Velde, U.Himmelreich	In vivo quantification of particle based and gene based MRI reporters in the rodent brain.	May 2011	Montreal, Canada	Scientists, Community Industry, Clinicians	5000	all
69	Conference	Ulf Ahlgren	Imaging the Pancreas, Minisymposium	12.11.2010	Umeå, Sweden	Scientists	100	all
70	Conference	Katja Werner	DiPIA – Developments in Protein Interaction Analysis 2010	17.10.2010	Barcelona, Spain	Scientists, Industry, Clinicians	400	all
71	Conference	Theo Schotten	ETP Nanomedicine General Assembly on Annual Forum 2010	14.10.2010	Milan, Italy	Scientists, Industry, EU project officers	300	EU
72	Conference	Ulf Ahlgren, Theo Schotten	Betalmage, EASD Pre-congress symposium on b-cell imaging	19.09.2010	Stockholm, Sweden	Scientists	1000	all
73	Conference	Berggren PO	46 <sup>th</sup> EASD Meeting	20.09.2010	Stockholm, Sweden	Scientists	2000	all
74	Conference	Joachim Thiem, Daniel Waschke	25 <sup>th</sup> International Carbohydrate Symposium (ICS 2010)	01.08.2010	Tokyo, Japan	Scientists	1000	all



75	Conference	Ulf Ahlgren	1st Islet society meeting	18.07.2010	Stockholm, Sweden	Scientists	200	all
76	Exhibition	Frank Schröder-Oeynhausen	NSTI 2010	21.06.2010	Anaheim, California, USA	Scientists, Community Industry,	3000	all
77	Conference	S.J.H. Soenen, U.Himmelreich	Intracellular iron oxide nanoparticle coating stability determines nanoparticle usability and cell functionality.	June 2010	Cardiff, Ireland	Scientists, Community, Industry, Clinicians	250	all
78	Workshop	Ahlgren U	5 <sup>th</sup> Workshop on visualisation of cells, tissues and animals by light and electron microscopy techniques and tomographic methods	25.05.2010	Oulu, Finland	Scientists	100	all
79	Exhibition	Theo Schotten	BIO Chicago 2010	02.05.2010	Chicago, Illinois, USA	Scientists, Industry	5000	all
80	Conference	S.J.H. Soenen, U.Himmelreich	The possible side-effects of iron oxide nanoparticles on cell functionality.	01.04.2010	Roma, Italy	Scientists, Community Industry, Clinicians	2000	all
81	Exhibition	Theo Schotten	Diabetes Messe Münster 2010 Invited Talk on VIBRANT	26.02.2010	Münster, Germany	Scientists, Patients, Industry, Clinicians	1000	all
82	Article	Schroeder-Oeynhausen	"DIE WELT" <a href="http://www.welt.de/die-welt/vermischtes/hamburg/article5719124/Die-Echse-Gilamonster-und-der-Kampf-gegen-Diabetes.html">http://www.welt.de/die-welt/vermischtes/hamburg/article5719124/Die-Echse-Gilamonster-und-der-Kampf-gegen-Diabetes.html</a>	04.01.2010		General Public	210000	130 countries
83	Conference	Schotten T	EuroNanoMedicine 2009, Bled, Slovenia	28.09.2009		Scientists, Industry	1000	all
84	Conference	U.Himmelreich	Can MRI provide non-invasive, high-resolution information on beta-cell mass and pancreatic islets in small animal models?	June 2009	Brussels, Belgium	Scientists, Industry, Clinicians	150	all
85	Article	Schroeder-Oeynhausen	TechPortal	<a href="http://www.techportal.de/de/0/0/news,public,newsdetail_public/1/start/,,,/1156/">http://www.techportal.de/de/0/0/news,public,newsdetail_public/1/start/,,,/1156/</a>		General Public	WWW	all

87	Article	Schroeder-Oeynhausen	Behörde für Wissenschaft und Forschung, City of Hamburg	<a href="http://www.hamburg.de/bwf/1633906/2009-07-24-bwf-nanomedizin.html">http://www.hamburg.de/bwf/1633906/2009-07-24-bwf-nanomedizin.html</a>		General Public	WWW	all
88	Article	Schroeder-Oeynhausen	CAN-Newsletter	<a href="http://www.can-hamburg.de/en/downloads/newsletter/Newsletter-2010-11-en.pdf">http://www.can-hamburg.de/en/downloads/newsletter/Newsletter-2010-11-en.pdf</a>		General Public	WWW	all
89	Article	Schroeder-Oeynhausen	CAN-Newsletter	<a href="http://www.can-hamburg.de/en/downloads/newsletter/Newsletter-2010-02-en.pdf">http://www.can-hamburg.de/en/downloads/newsletter/Newsletter-2010-02-en.pdf</a>		General Public	WWW	all
90	Article	Schroeder-Oeynhausen	CAN-Newsletter	<a href="http://www.can-hamburg.de/en/downloads/newsletter/Newsletter-2009-09-en.pdf">http://www.can-hamburg.de/en/downloads/newsletter/Newsletter-2009-09-en.pdf</a>		General Public	WWW	all

**Section B (Confidential<sup>2</sup> or public: confidential information to be marked clearly)**  
**Part B1**

The applications for patents, trademarks, registered designs, etc. shall be listed according to the template B1 provided hereafter.

The list should, specify at least one unique identifier e.g. European Patent application reference. For patent applications, only if applicable, contributions to standards should be specified. This table is cumulative, which means that it should always show all applications from the beginning until after the end of the project.

<b>TEMPLATE B1: LIST OF APPLICATIONS FOR PATENTS, TRADEMARKS, REGISTERED DESIGNS, ETC.</b>					
Type of IP Rights <sup>3</sup> :	Confidential Click on YES/NO	Foreseen embargo date dd/mm/yyyy	Application reference(s) (e.g. EP123456)	Subject or title of application	Applicant (s) (as on the application)
Patent Application	NO	NA	EP2414091 (A1)	Method and apparatus for the manufacture of a colloidal dispersion using controlled micro-channel flow	Förster S., Barkmann C., Schotten T.
Patent Application	NO	NA	WO2012016935 (A1)	Novel Seven Carbon (C-7) Sugars, Derivatives and Their Use	Leshch Y., Waschke D., Thimm J., Thiem J., Malaisse W.J., Louchami K.
Patent Application	NO	NA	WO2012001012 (A2)	A micellular combination comprising a nanoparticle and a plurality of surfmer ligands	Pöselt, E., Schmidtke C., Fischer S., Kloust H., Weller H., Schotten T., et al

---

<sup>2</sup> Note to be confused with the "EU CONFIDENTIAL" classification for some security research projects.

<sup>3</sup> A drop down list allows choosing the type of IP rights: Patents, Trademarks, Registered designs, Utility models, Others.

## Part B2

Please complete the table hereafter:

Type of Exploitable Foreground <sup>4</sup>	Description of exploitable foreground	Confidential Click on YES/NO	Foreseen embargo date dd/mm/yyyy	Exploitable product(s) or measure(s)	Sector(s) of application <sup>5</sup>	Timetable, commercial or any other use	Patents or other IPR exploitation (licences)	Owner & Other Beneficiary(s) involved
Commercial exploitation of R&D results	Fluorescent quantum dots	NO	NA	CANdots Series A	Life Science, Displays	2010	Patents filed Trade Secrets	Beneficiary CAN GmbH (owner) Beneficiary Univ Hamburg Distribution via supplier STREM Chemicals Inc.,
Commercial exploitation of R&D results	Superparamagnetic Iron Oxide Nanoparticles	NO	NA	CANdots Series M	Life Science	2013	Patents filed Trade Secrets	Beneficiary CAN GmbH (owner) Beneficiary Univ Hamburg,
Commercial exploitation of R&D results	Plasmonic Gold Nanoparticles	NO	NA	CANdots Series G, CAN HisDetect, Kits	Life Science, in vitro Diagnostics	2012	Trade Secret	Beneficiary CAN GmbH (owner) Distribution via supplier AppliChem
Commercial exploitation of R&D results	Fluororous Phase Nanoparticles	YES	01/09/2014	CANdots Series Fluorine	Life Science, preclinical MRI Diagnostics	2014	Trade Secret Patent application feasible	Beneficiary CAN GmbH (owner) Beneficiary Katholieke Univ Leuven

<sup>19</sup> A drop down list allows choosing the type of foreground: General advancement of knowledge, Commercial exploitation of R&D results, Exploitation of R&D results via standards, exploitation of results through EU policies, exploitation of results through (social) innovation.

<sup>5</sup> A drop down list allows choosing the type sector (NACE nomenclature) : [http://ec.europa.eu/competition/mergers/cases/index/nace\\_all.html](http://ec.europa.eu/competition/mergers/cases/index/nace_all.html)

General advancement of knowledge	Synthesis and biofunctionalization of highly stable fluorescent, superparamagnetic, or hybrid nanoparticles	NO	NA	Publications, Contract research, Industrial Collaborations	Scientific Community	2009 ongoing	WO201200101 (A2)	Beneficiary Univ Hamburg (owner), Beneficiary CAN GmbH
General advancement of knowledge	Synthesis of biodegradable polyester nanocapsules for drug delivery	YES	01/09/2015	Publications, Contract research, Industrial Collaborations	Scientific Community, Drug Industry	2015	Trade Secret Patent application feasible	Beneficiary Univ Bayreuth (owner), Beneficiary CAN GmbH
General advancement of knowledge	Synthesis of Seven carbon Sugars and Derivatives (AJ070)	YES	01/09/2015	Publications, Industrial Collaborations Specific Contrast Agent (preclinical)	Scientific Community, Drug Industry	2015	Trade Secret Patent application feasible, Under evaluation	Beneficiary Univ Hamburg (owner) Beneficiary CAN GmbH Beneficiary Karolinska Institute
General advancement of knowledge	High Content Screen on Insulin Producing Cells (xCelligence Platform)	NO	NA	Publications, Contract research, Industrial Collaborations	Scientific Community, Drug Industry	2013	NA	Beneficiary Univ Copenhagen (owner)
Commercial exploitation of R&D results	Use of Fluorinated Sugars as MRI Contrast Agents	NO	NA	Publications, Contract research, Industrial Collaborations	Scientific Community, Drug Industry		WO2012016935A1	Beneficiary Univ Brussels (owner) Beneficiary Univ Hamburg (owner) Beneficiary CAN GmbH, Beneficiary Katholieke Univ Leuven

<i>Commercial exploitation of R&amp;D results</i>	<i>Encapsulation Process</i>	NO	NA	<i>Contract research, Industrial Collaborations</i>	<i>Scientific Community, Drug Industry</i>	2013	<i>EP2414091 (A1)</i>	<i>Beneficiary CAN GmbH (owner), Beneficiary Univ Bayreuth</i>
<i>General advancement of knowledge</i>	<i>19F-MRI Methods</i>	YES		<i>Publications, Contract research, Industrial Collaborations</i>	<i>Scientific Community, Drug Industry</i>	2013		<i>Beneficiary Katholike Univ Leuven (owner) Beneficiary CAN GmbH</i>
<i>General advancement of knowledge</i>	<i>T2/T2*MRI Methods</i>			<i>Publications, Contract research, Industrial Collaborations</i>	<i>Scientific Community, Drug Industry</i>	2013		<i>Beneficiary Katholike Univ Leuven (owner) Beneficiary Umea Univ Beneficiary Univ Hamburg</i>
<i>General advancement of knowledge</i>	<i>MRI on Eye</i>	NO	NA	<i>Publications, Contract research, Industrial Collaborations</i>	<i>Scientific Community, Drug Industry</i>	2013		<i>Beneficiary Katholike Univ Leuven (owner) Beneficiary Karolinska Institute (owner)</i>
<i>General advancement of knowledge</i>	<i>Functional 3D-MRI of pancreas by Mn2+</i>	NO	NA	<i>Publications</i>	<i>Scientific Community,</i>	2013		<i>Beneficiary Univ. Bremen (owner)</i>



<i>General advancement of knowledge</i>	<i>Improved Cell labeling with Magneto Liposomes</i>	YES	01/09/2016	<i>Publications</i>	<i>Scientific Community, Clinical Development</i>	2013	<i>Under evaluation</i>	<i>Beneficiary Katholieke Univ Leuven (owner), Beneficiary CAN GmbH</i>
<i>Commercial exploitation of R&amp;D results</i>	<i>Fluorescent Quantum Dots for labeling of histological tissue sections</i>	YES	01/09/2015	<i>Labeling Kits</i>	<i>Life Science Ex vivo Diagnostics</i>	2015	<i>Under evaluation</i>	<i>Beneficiary CAN GmbH (owner)</i>
<i>Commercial exploitation of R&amp;D results</i>	<i>Novel mesoscopic imaging by OPTiSPIM</i>	YES	01/09/2015	<i>Instrument</i>	<i>Life Science Ex vivo Diagnostics</i>	2015	<i>Under evaluation</i>	<i>Beneficiary Umea Univ. and Center for Genetic Regulation, Barcelona (owner), Poss. licensing to BIOPTONICS</i>
<i>General advancement of knowledge</i>	<i>Novel MRI/OPTiSPIM crossvalidation methodology</i>	NO	NA	<i>Publications</i>	<i>Scientific Community</i>	2013		<i>Beneficiary Umea Univ. and Center for Genetic Regulation, Barcelona (owner)</i>
<i>Commercial exploitation of R&amp;D results</i>	<i>Crossvalidation by NIR-labeled SPIOs</i>	YES	01/09/2015	<i>Labeling Kits</i>	<i>Scientific Community, Life Science Industry</i>	2015	<i>Under evaluation</i>	<i>Beneficiary CAN GmbH (owner) Beneficiary Umea Univ., Beneficiary Katholieke Univ Leuven</i>

In addition to the table, please provide a text to explain the exploitable foreground, in particular:

- Its purpose
- How the foreground might be exploited, when and by whom
- IPR exploitable measures taken or intended
- Further research necessary, if any
- Potential/expected impact (quantify where possible)

**In summary, VIBRANT provided comprehensive technology for the manufacturing of nanoparticulate probes, bearing biological recognition motifs, for multi-modal imaging and drug-delivery. Superparamagnetic iron oxide NCs were highly sensitive for the detection of single islets and superior to commercial materials. The fluorophore phase MRI agents developed, offer new opportunities for improved imaging modalities.**

**Knowledge on  $\beta$ -cell function, survival and regeneration was substantially expanded. During VIBRANT, highly sophisticated *in vitro* assays and *in vivo* models were developed and adapted to MRI. An independent cross-validation of the MRI results was accomplished by OPT.  $Mn^{2+}$ -enhanced MRI can detect small changes in functional  $\beta$ -cells *in vivo* and is a potential method for early noninvasive detection of changes in functional  $\beta$ -cell mass.**

**Unfortunately, -at the time- *in vivo*  $\beta$ -cell imaging by means of nanoparticulate probes was not achievable, possibly due to insufficient  $\beta$ -cell affinity of the selected ligands. However, search for novel high-affinity ligands was not in the scope of VIBRANT. Once as such will become available, studies should be resumed, because all technical success factors have been developed. In particular, surrogate proof-of-principle studies clearly indicate feasibility of anatomical and functional pancreatic  $\beta$ -cell imaging and quantification of BCM. Promisingly, a small molecule fluorescent carbohydrate derivative AJ 070 showed specific labeling of islets *in vitro* and *in vivo* and will be further pursued**

## **NANOPARTICLE MANUFACTURING**

Within VIBRANT, different kinds of nanoparticles have been developed and optimized for putative labeling of  $\beta$ -cells, but eventually will find broad application in preclinical biomedical applications in general.

### **Fluorescent Quantum Dots**

Premium, highly reproducible semiconductor fluorescent nanoparticles (quantum dots) are provided by CAN GmbH via a highly reproducible proprietary continuous flow process and are worldwide distributed via STREM Chemicals INC under the trademark CANdots Series A. QDs find increasing applications in solar and fuel cells, as markers in life science and in displays. See: <http://www.can-hamburg.de/english/menu/products/candots-series-a.html>. During the last decade, considerable efforts have been made in order to exploit the unique spectral properties of fluorescent nanocrystals -so-called semiconductor quantum dots (QDs) - in biological and preclinical applications. In particular, absorption and emission wavelengths of QDs are size-tuneable, providing extremely broad and intense absorption bands, very narrow emission bands and high fluorescence quantum yields. Conventional synthetic routes via batch processes suffer from poor size control, hence resulting in undesirable broadening of emission bands. Partner 1 (CAN GmbH) developed and optimized a proprietary continuous flow synthesis, providing superior control and reproducibility of the semiconductor core materials. As a result, these QDs are now commercialized under the trademark CANdots Series A ® and distributed by STREM Chemicals Inc.

Since QDs are hydrophobic after synthesis in high boiling organic solvents, a surface modification has to be done to render them water-soluble and biocompatible, without compromising the spectral properties. To this end, several different, often polymeric ligand systems have been developed. An optimized ligand system will provide superior colloidal stability in biological media, as well as high fluorescence quantum yields for extended periods. Additionally, particles will be straightforwardly functionalized. Both aims – facile

functionalization and protection against quenching – are still major challenges. Within VIBRANT these goals have been fully achieved by partner 2 (UH, Weller group) by polymer encapsulation, providing highly fluorescent, functionalized nanocontainers with excellent stability and very low toxicity in biological media in vitro and in vivo. Furthermore, the probes show unrivalled stability against chemicals, frequently used in histology for tissue preparations, making them highly suitable for specific histological stainings. Finally, these probes will spur progress in life science and preclinical applications.

A novel series of fluorescent QD, developed by partner 2 (Weller group) show unrivalled stability against chemicals, frequently used in histology for tissue preparations, making them highly suitable for specific histological stainings. These particles will be further developed and commercialized by partner 1 (CAN GmbH), either as commodities for the life science community or in ex vivo diagnostic kits, e.g. for staining of intra-operative quick sections. Finally, these probes will spur progress in life science and preclinical applications.

### **Superparamagnetic Iron Oxide Nanoparticles (SPIOs)**

Superparamagnetic nanoparticles are suitable for all applications where homogeneously dispersed particles with only one magnetic domain are needed. They exhibit the following properties:

- Diameter of the particles tunable between 5 and 25 nm
- Small size distribution due to high temperature synthesis
- Superparamagnetism up to a particle diameter of 20 nm
- High stability against heat or exposure to light
- Homogeneously dispersible in non polar or aqueous media
- Water soluble particles can be delivered with functional groups like NH<sub>2</sub> for coupling to affinity molecules?

CANDot Series M particles consist of an iron oxide core surrounded by a layer of oleic acid molecules to prevent agglomeration and to enable a homogeneous dispersion in non polar media like n-hexane. For the use in biomedical research these particles are also available with a PEG coating to allow their dispersibility in water or buffer. Using the functional groups at the outside it is further possible to attach affinity molecules to these particles. See:

<http://www.can-hamburg.de/english/menu/products/candots-series-m.html>.

Inorganic nanocrystals are well-established in biological and medical applications.<sup>1</sup> Especially the superparamagnetic iron oxide nanocrystals are of great interest and find application as contrast agents for T<sub>2</sub>- or T<sub>2</sub>\*-, and recently even T<sub>1</sub>-weighted magnetic resonance imaging (MRI). The SPIOs developed during VIBRANT are highly sensitive for the detection of even single islets and superior to commercial materials in all aspects, as demonstrated by partner 9 (KULeuven). Additionally, protocols for the controlled clustering have been developed for optimized magnetic relaxivities. The SPIO-nanocontainers, as well as the associated technology will be further exploited in ongoing third party collaborations.

### **Plasmonic Gold nanoparticles**

Plasmonic nanoparticles for optical read-out in applications in the visible wavelength range. Gold nanoparticles exhibit an intensive red colour in aqueous dispersions caused by the so called localized surface plasmon resonance (LSPR). The extremely high extinction coefficient in combination with the ease of biofunctionalization renders CANDots® Series G ideally for the generation of selective molecular markers (up to 5 orders of magnitude higher

sensitivity than fluorescence-based detection techniques) e.g. for use in immunoassays. A quantitative assay read-out via absorption intensity is feasible,; See: <http://www.can-hamburg.de/english/menu/products/candots-series-g.html>. Albeit not in the original focus of VIBRANT, plasmonic gold nanoparticles were used as gauges for the endothelial fenestration of islets. During VIBRANT, gold NPs were developed marketable and are currently commercialized in conjugation kits, distributed by AppliChem.

### **Fluorous Phase Nanocontainers**

Stable Fluorous Phase Nanoparticles are a novel development. Currently, for  $^{19}\text{F}$ -MRI emulsions of perfluorinated agents are used. The preparations show limited stability, adhere unspecifically to tissues and cannot be functionalized for targeted delivery.  $^{19}\text{F}$ -MRI is a quite recent concept for preclinical imaging. The main advantages is a hyperintense contrast, which is less prone to artifacts, can be quantified, and can be superimposed with anatomical images from  $^1\text{H}$ -MRI. Promising results have been shown for islet labeling. Hitherto, microemulsions of fluorine compounds suffered from low stability and high background due to unspecific cellular binding. Functionalization was unsatisfactory. Within VIBRANT, novel fluorous phase nanocontainers have been accomplished, which resolve these issues. A novel encapsulation process was developed and used in collaboration with partner 11 (Univ. Bayreuth). Further development will be needed from partners 1 and 9. The results will be confidential until patentability is evaluated. The fluorous phase nanocontainers and associated  $^{19}\text{F}$  imaging technology, developed by partner 9 (KULeuven) bear high potential in preclinical research.

### **Hybrid Nanocontainers**

Stability of nanoparticles in biological environments is a delicate issue. The methods developed within VIBRANT as cited in the publication list attached (Weller group) constitute major progress in this field and will spur further developments. The concept of inorganic hybrid nanostructures is to combine the disparate physico chemical properties of diverse nanocrystals towards higher integrated functionalities, affording diagnostic modalities, otherwise not obtainable with the discrete nanomaterials. Undeniably, different kinds of nanoparticles should fully maintain, rather than mutually compromise their original properties, resulting in e.g. undesirable fluorescence quenching, energy transfer, or concurring light absorption processes, due to the proximity of fluorescent components to the other materials. Within VIBRANT, partner 2 (Weller group) succeeded in providing optimized magneto-fluorescent, as well as fluorescent F-phase nanocontainers for multimodal imaging. Furthermore, partner 1 accomplished superparamagnetic NIR probes for independent cross validation of biological specimens via MRI and NIR scanning, as demonstrated by partners 6 (Umea Univ.), 7 (CRG) and 9 (KULeuven). This concept requires additional research until commercial exploitation.

### **Hybrid NIR-SPIOs**

Partner 1 (Can GmbH) prepared SPIO-NCs conjugated to a NIR dyestuff. These hybrid nanoconstructs proved to be suitable for multimodal imaging, namely T2/T2\*MRI, OPT, and Fluorescence Imaging. Biofunctionalization with antibodies or peptides was accomplished as well. Hence, these new hybrid nanoconstructs hold high potential as customized probes for the life science and preclinical imaging community. Exploitation will be pursued by partner 1 by contract research and services.

## **Biodegradable Polyester nanocontainers for Drug Delivery**

The biodegradable polyester nanocapsules prepared within VIBRANT are applicable for drug delivery and controlled release. This concept is of high interest in the pharmaceutical industry. Nanocontainers, which could be functionalized with affinity molecules and enclose a lipophilic payload, e.g. JNK-inhibitor SP600125 (1,9-Pyrazoloanthrone), as demonstrated in a proof-of-principle study together with partner 10 (Univ. Bremen). However, albeit very promising, considerable research will be required to further apply the concept in practice.

## **Magnetoliposomes**

Partner 9 (KULeuven) succeeded in the encapsulation of premium quality SPIOs provided by partner 1 (CAN) into phospholipid liposomes, which were highly suitable for cell labeling, because of their low toxicity, better uptake, and high signal intensity, hence superior to conventional agents. A product development for the scientific life science community appears feasible

## **Fluorinated 7-carbon Sugars**

The fluorinated 7-carbon sugars were selectively uptaken by various cells and can be used as cellular labels in 19F-MRI. Details are reported in the patent application WO2012016935 (A1). For the further development partnering with the drug industry is required.

## **Fluorescent 7-carbon Sugars**

The 7-carbon sugars were selectively uptaken by various cells and can be either used as cellular labels after conjugation to dyestuffs for optical read-outs. This is of interest for diagnostic applications. A patent application is under evaluation. Partner 2 (Univ. Hamburg, J.Thiem) synthesized manno- and glucoheptulose derivatives, optionally conjugated to a fluorescent label. Remarkably, such a conjugate, namely AJ070 showed fluorescent labeling of islets in vitro and in vivo in models provided by partner 4 (Karolinska Institute). Because of their potential, these experiments will be pursued further after the end of VIBRANT. After positive validation, such a reagent will be of major impact for functional and anatomical  $\beta$ -cell imaging. Currently, the results will be kept confidential. After validation, protection of IPR in a patent application will be pursued. Further development will be done in collaboration with the pharmaceutical industry.

## **METHODS**

### **Testing NCs for toxicity on INS1 cell line using the xCELLigence platform**

By adapting a commercial cell analyzer xCelligence (Roche) to insulin secreting cell lines (INS1) Partner 12 (Univ. Copenhagen) developed a high content/high capacity screen for toxicity and biological response of effectors and nanoparticulate probes. This highly predictive screening could be of considerable interest for the pharmaceutical industry for the development of anti-diabetic drugs. A further development is under evaluation. Remarkably, a NC conjugate to GLP1 (EU-0533) showed a unique proliferative effect on INS1 cells at concentrations of up to 100nM. Binding to INS1 cells was proven by fluorescence microscopy. Further research is required for validation of these findings.

## **Islet Transplants in the Anterior Chamber of the Eye**

When transplanted into the anterior chamber of the eye, pancreatic islets become fully vascularized and innervated. These engrafted islets reflect exactly the status of endogenous islets, thus key aspects of  $\beta$ -cell morphology and function can be studied noninvasively using in vivo imaging techniques, due to the ideal optical and structural properties of the eye. The ACE model also offers a unique opportunity to noninvasively detect and visualize fluorescent NCs in islet transplants. In addition to the development of techniques allowing in vitro screening of functionalized fluorescent NCs for their specific binding to  $\beta$ -cells, the ACE model permits to assess their potential binding properties under in vivo conditions. This unique method was introduced as background of partner 4 (Karolinska Institute), and is of great potential for diagnostic and therapeutic applications in diabetes management. Partner 9 accomplished an adaptation of this sophisticated model to MRI monitoring in combination with fluororous phase nanocontainers. This method holds high potential for the scientific community and will be further pursued in research collaborations.

### **$Mn^{2+}$ -enhanced MRI for the detection of small changes in functional $\beta$ -cells *in vivo***

In order to monitor  $\beta$ -cell survival and function in vivo, a robust 3D MR imaging of the mouse abdomen by using  $Mn^{2+}$  ions was established by partner 10 (Uni Bremen). Manganese ions display similar properties as calcium, but in contrast are paramagnetic, thus allowing MRI. Consequently, analysis of  $\beta$ -cell function/ mass and measurement techniques of the mouse abdomen with manganese in 2 animal models of diabetes were accomplished.  $Mn^{2+}$ -enhanced MRI can detect small changes in functional  $\beta$ -cells in vivo and is a potential method for early noninvasive detection of changes in functional  $\beta$ -cell mass.

## **Integration of SPIM into the OPT setup and high-resolution mesoscopic analyses and co-registration of OPT and MRI**

Optical Projection Tomography (OPT) imaging currently provides the highest resolution available for whole organ ex vivo imaging of islets in intact pancreata. Further, the cell-level resolution imaging technique Selective Plane Illumination Microscopy (SPIM) has been integrated into the OPT setup. By combination of these two mesoscopic imaging techniques (OPT and SPIM) in one single setup a worldwide unique instrument was generated by partners 6 (Umea Univ.) and 7 (Centre of Genomic Regulation, Barcelona). Imaging with the new setup showed a significant higher resolution and detail in its sub-tiles compared to data that was acquired previously by OPT. The instrument, together with the associated technology will be exploited by the inventor's spin-off (Bioptonics).

The method was further adapted for the cross-validation of MRI studies, demonstrated by pre-labeling of pancreata with magneto-fluorescent nanoparticles, provided by partner 1. This method, enabled by the tissue clearing protocols developed by partner 6, holds very high potential to set new standards for the independent cross-validation of imaging studies in general.

New image processing assisted algorithms for OPT were developed by partner 7 (Umea Univ.) that generally contribute to increase acquisition speed and quality of pancreatic OPT data. More specifically this included 1) algorithms for semi-automatic and precise positioning



of a sample at the axis of rotation, 2) a fast and robust algorithm for determination of post alignment values throughout the specimen as compared to existing methods , and 3) a computational statistical approach implementing the concept of contrast limited adaptive histogram equalisation (CLAHE). The latter approach significantly increases both, the sensitivity of OPT for islet imaging and the conservation of islet morphology. This contribution will be exploited in the context of the OPTiSPIM instrument, developed by partner 7 (CGR) and their spin-off (BIOPTONICS)

## Report on societal implications

Replies to the following questions will assist the Commission to obtain statistics and indicators on societal and socio-economic issues addressed by projects. The questions are arranged in a number of key themes. As well as producing certain statistics, the replies will also help identify those projects that have shown a real engagement with wider societal issues, and thereby identify interesting approaches to these issues and best practices. The replies for individual projects will not be made public.

### **A General Information** *(completed automatically when Grant Agreement number is entered.*

Grant Agreement Number:

228933

Title of Project:

VIBRANT

Name and Title of Coordinator:

Theo Schotten PhD

### **B Ethics**

#### **1. Did your project undergo an Ethics Review (and/or Screening)?**

- If Yes: have you described the progress of compliance with the relevant Ethics Review/Screening Requirements in the frame of the periodic/final project reports?

**NO**

Special Reminder: the progress of compliance with the Ethics Review/Screening Requirements should be described in the Period/Final Project Reports under the Section 3.2.2 'Work Progress and Achievements'

#### **2. Please indicate whether your project involved any of the following issues (tick box) :**

##### **RESEARCH ON HUMANS**

• Did the project involve children?	NO
• Did the project involve patients?	NO
• Did the project involve persons not able to give consent?	NO
• Did the project involve adult healthy volunteers?	NO
• Did the project involve Human genetic material?	NO
• Did the project involve Human biological samples?	NO
• Did the project involve Human data collection?	NO

##### **RESEARCH ON HUMAN EMBRYO/FOETUS**

• Did the project involve Human Embryos?	NO
• Did the project involve Human Foetal Tissue / Cells?	NO

• Did the project involve Human Embryonic Stem Cells (hESCs)?	NO
• Did the project on human Embryonic Stem Cells involve cells in culture?	NO
• Did the project on human Embryonic Stem Cells involve the derivation of cells from Embryos?	NO
<b>PRIVACY</b>	
• Did the project involve processing of genetic information or personal data (eg. health, sexual lifestyle, ethnicity, political opinion, religious or philosophical conviction)?	NO
• Did the project involve tracking the location or observation of people?	NO
<b>RESEARCH ON ANIMALS</b>	
• Did the project involve research on animals?	YES
• Were those animals transgenic small laboratory animals?	NO
• Were those animals transgenic farm animals?	NO
• Were those animals cloned farm animals?	NO
• Were those animals non-human primates?	NO
<b>RESEARCH INVOLVING DEVELOPING COUNTRIES</b>	
• Did the project involve the use of local resources (genetic, animal, plant etc)?	NO
• Was the project of benefit to local community (capacity building, access to healthcare, education etc)?	NO
<b>DUAL USE</b>	
• Research having direct military use	NO
• Research having the potential for terrorist abuse	NO

## C Workforce Statistics

### 3. Workforce statistics for the project: Please indicate in the table below the number of people who worked on the project (on a headcount basis).

Type of Position	Number of Women	Number of Men
Scientific Coordinator	0	1
Work package leaders	2	8
Experienced researchers (i.e. PhD holders)	14	16
PhD Students	21	22
Other	15	3

4. How many additional researchers (in companies and universities) were recruited specifically for this project?	12
Of which, indicate the number of men:	4

<b>D Gender Aspects</b>			
<b>5. Did you carry out specific Gender Equality Actions under the project?</b>	X ○	Yes No	
<b>6. Which of the following actions did you carry out and how effective were they?</b>			
	Not at all effective	Very effective	
○ Design and implement an equal opportunity policy	○ ○ ○	X ○	
○ Set targets to achieve a gender balance in the workforce	○ ○ ○	X ○	
○ Organise conferences and workshops on gender	○ X ○ ○ ○		
○ Actions to improve work-life balance	○ ○ ○	X ○	
○ Other: <span style="border: 1px solid black; display: inline-block; width: 300px; height: 20px; vertical-align: middle;"></span>			
<b>7. Was there a gender dimension associated with the research content – i.e. wherever people were the focus of the research as, for example, consumers, users, patients or in trials, was the issue of gender considered and addressed?</b>			
○ Yes- please specify <span style="border: 1px solid black; display: inline-block; width: 150px; height: 20px; vertical-align: middle;"></span>			
X No			
<b>E Synergies with Science Education</b>			
<b>8. Did your project involve working with students and/or school pupils (e.g. open days, participation in science festivals and events, prizes/competitions or joint projects)?</b>			
○ Yes- please specify <span style="border: 1px solid black; display: inline-block; width: 150px; height: 20px; vertical-align: middle;"></span>			
X No			
<b>9. Did the project generate any science education material (e.g. kits, websites, explanatory booklets, DVDs)?</b>			
○ Yes- please specify <span style="border: 1px solid black; display: inline-block; width: 150px; height: 20px; vertical-align: middle;"></span>			
X No			
<b>F Interdisciplinarity</b>			
<b>10. Which disciplines (see list below) are involved in your project?</b>			
○ Main discipline <sup>6</sup> : 2.3			
○ Associated discipline <sup>6</sup> : 1.2, 1.3, 1.5	○	Associated discipline <sup>6</sup> : 3.1; 3.2	
<b>G Engaging with Civil society and policy makers</b>			
<b>11a Did your project engage with societal actors beyond the research community? (if 'No', go to Question 14)</b>	○ X	Yes No	
<b>11b If yes, did you engage with citizens (citizens' panels / juries) or organised civil society (NGOs, patients' groups etc.)?</b>			
○ No			
○ Yes- in determining what research should be performed			
○ Yes - in implementing the research			
○ Yes, in communicating /disseminating / using the results of the project			

<sup>6</sup> Insert number from list below (Frascati Manual).

<b>11c In doing so, did your project involve actors whose role is mainly to organise the dialogue with citizens and organised civil society (e.g. professional mediator; communication company, science museums)?</b>		<input type="radio"/> <input type="radio"/>	Yes No
<b>12. Did you engage with government / public bodies or policy makers (including international organisations)</b>			
<input type="radio"/> No <input type="radio"/> Yes- in framing the research agenda <input type="radio"/> Yes - in implementing the research agenda <input type="radio"/> Yes, in communicating /disseminating / using the results of the project			
<b>13a Will the project generate outputs (expertise or scientific advice) which could be used by policy makers?</b> <input type="radio"/> Yes – as a <b>primary</b> objective (please indicate areas below- multiple answers possible) <input type="radio"/> Yes – as a <b>secondary</b> objective (please indicate areas below - multiple answer possible) <input checked="" type="radio"/> No			
<b>13b If Yes, in which fields?</b>			
Agriculture Audiovisual and Media Budget Competition Consumers Culture Customs Development Economic and Monetary Affairs Education, Training, Youth Employment and Social Affairs		Energy Enlargement Enterprise Environment External Relations External Trade Fisheries and Maritime Affairs Food Safety Foreign and Security Policy Fraud Humanitarian aid	Human rights Information Society Institutional affairs Internal Market Justice, freedom and security Public Health Regional Policy Research and Innovation Space Taxation Transport

<b>13c If Yes, at which level?</b> <input type="radio"/> Local / regional levels <input type="radio"/> National level <input type="radio"/> European level <input type="radio"/> International level										
<b>H Use and dissemination</b>										
<b>14. How many Articles were published/accepted for publication in peer-reviewed journals?</b>	<b>56</b>									
<b>To how many of these is open access<sup>7</sup> provided?</b>	<b>12</b>									
<b>How many of these are published in open access journals?</b>	<b>120</b>									
<b>How many of these are published in open repositories?</b>	<b>0</b>									
<b>To how many of these is open access not provided?</b>	<b>44</b>									
<b>Please check all applicable reasons for not providing open access:</b>										
<input checked="" type="checkbox"/> publisher's licensing agreement would not permit publishing in a repository <input type="checkbox"/> no suitable repository available <input checked="" type="checkbox"/> no suitable open access journal available <input checked="" type="checkbox"/> no funds available to publish in an open access journal <input checked="" type="checkbox"/> lack of time and resources <input checked="" type="checkbox"/> lack of information on open access <input type="checkbox"/> other <sup>8</sup> : .....										
<b>15. How many new patent applications ('priority filings') have been made?</b> <i>("Technologically unique": multiple applications for the same invention in different jurisdictions should be counted as just one application of grant).</i>	<b>3</b>									
<b>16. Indicate how many of the following Intellectual Property Rights were applied for (give number in each box).</b>	Trademark	<b>0</b>								
	Registered design	<b>0</b>								
	Other	<b>0</b>								
<b>17. How many spin-off companies were created / are planned as a direct result of the project?</b>	<b>0</b>									
<i>Indicate the approximate number of additional jobs in these companies:</i>		<b>NA</b>								
<b>18. Please indicate whether your project has a potential impact on employment, in comparison with the situation before your project:</b> <table border="0"> <tr> <td><input checked="" type="checkbox"/> Increase in employment, or</td> <td><input checked="" type="checkbox"/> In small &amp; medium-sized enterprises</td> </tr> <tr> <td><input checked="" type="checkbox"/> Safeguard employment, or</td> <td><input type="checkbox"/> In large companies</td> </tr> <tr> <td><input type="checkbox"/> Decrease in employment,</td> <td><input type="checkbox"/> None of the above / not relevant to the project</td> </tr> <tr> <td><input type="checkbox"/> Difficult to estimate / not possible to quantify</td> <td></td> </tr> </table>			<input checked="" type="checkbox"/> Increase in employment, or	<input checked="" type="checkbox"/> In small & medium-sized enterprises	<input checked="" type="checkbox"/> Safeguard employment, or	<input type="checkbox"/> In large companies	<input type="checkbox"/> Decrease in employment,	<input type="checkbox"/> None of the above / not relevant to the project	<input type="checkbox"/> Difficult to estimate / not possible to quantify	
<input checked="" type="checkbox"/> Increase in employment, or	<input checked="" type="checkbox"/> In small & medium-sized enterprises									
<input checked="" type="checkbox"/> Safeguard employment, or	<input type="checkbox"/> In large companies									
<input type="checkbox"/> Decrease in employment,	<input type="checkbox"/> None of the above / not relevant to the project									
<input type="checkbox"/> Difficult to estimate / not possible to quantify										
<b>19. For your project partnership please estimate the employment effect resulting directly from your participation in Full Time Equivalent (FTE = one person working fulltime for a year) jobs:</b>	<i>Indicate figure:</i>									

<sup>7</sup> Open Access is defined as free of charge access for anyone via Internet.

<sup>8</sup> For instance: classification for security project.

Difficult to estimate / not possible to quantify	X												
<b>I Media and Communication to the general public</b>													
<b>20. As part of the project, were any of the beneficiaries professionals in communication or media relations?</b> <input type="radio"/> Yes <input checked="" type="radio"/> No													
<b>21. As part of the project, have any beneficiaries received professional media / communication training / advice to improve communication with the general public?</b> <input type="radio"/> Yes <input checked="" type="radio"/> No													
<b>22 Which of the following have been used to communicate information about your project to the general public, or have resulted from your project?</b> <table border="1"> <tr> <td><input checked="" type="checkbox"/> Press Release</td> <td><input checked="" type="checkbox"/> Coverage in specialist press</td> </tr> <tr> <td><input type="checkbox"/> Media briefing</td> <td><input type="checkbox"/> Coverage in general (non-specialist) press</td> </tr> <tr> <td><input type="checkbox"/> TV coverage / report</td> <td><input checked="" type="checkbox"/> Coverage in national press</td> </tr> <tr> <td><input checked="" type="checkbox"/> Radio coverage / report</td> <td><input checked="" type="checkbox"/> Coverage in international press</td> </tr> <tr> <td><input checked="" type="checkbox"/> Brochures /posters / flyers</td> <td><input checked="" type="checkbox"/> Website for the general public / internet</td> </tr> <tr> <td><input type="checkbox"/> DVD /Film /Multimedia</td> <td><input checked="" type="checkbox"/> Event targeting general public (festival, conference, exhibition, science café)</td> </tr> </table>		<input checked="" type="checkbox"/> Press Release	<input checked="" type="checkbox"/> Coverage in specialist press	<input type="checkbox"/> Media briefing	<input type="checkbox"/> Coverage in general (non-specialist) press	<input type="checkbox"/> TV coverage / report	<input checked="" type="checkbox"/> Coverage in national press	<input checked="" type="checkbox"/> Radio coverage / report	<input checked="" type="checkbox"/> Coverage in international press	<input checked="" type="checkbox"/> Brochures /posters / flyers	<input checked="" type="checkbox"/> Website for the general public / internet	<input type="checkbox"/> DVD /Film /Multimedia	<input checked="" type="checkbox"/> Event targeting general public (festival, conference, exhibition, science café)
<input checked="" type="checkbox"/> Press Release	<input checked="" type="checkbox"/> Coverage in specialist press												
<input type="checkbox"/> Media briefing	<input type="checkbox"/> Coverage in general (non-specialist) press												
<input type="checkbox"/> TV coverage / report	<input checked="" type="checkbox"/> Coverage in national press												
<input checked="" type="checkbox"/> Radio coverage / report	<input checked="" type="checkbox"/> Coverage in international press												
<input checked="" type="checkbox"/> Brochures /posters / flyers	<input checked="" type="checkbox"/> Website for the general public / internet												
<input type="checkbox"/> DVD /Film /Multimedia	<input checked="" type="checkbox"/> Event targeting general public (festival, conference, exhibition, science café)												
<b>23 In which languages are the information products for the general public produced?</b> <table border="1"> <tr> <td><input checked="" type="checkbox"/> Language of the coordinator</td> <td><input checked="" type="checkbox"/> English</td> </tr> <tr> <td><input type="checkbox"/> Other language(s)</td> <td></td> </tr> </table>		<input checked="" type="checkbox"/> Language of the coordinator	<input checked="" type="checkbox"/> English	<input type="checkbox"/> Other language(s)									
<input checked="" type="checkbox"/> Language of the coordinator	<input checked="" type="checkbox"/> English												
<input type="checkbox"/> Other language(s)													

**Question F-10:** Classification of Scientific Disciplines according to the Frascati Manual 2002 (Proposed Standard Practice for Surveys on Research and Experimental Development, OECD 2002):

## **FIELDS OF SCIENCE AND TECHNOLOGY**

### 1. NATURAL SCIENCES

- 1.1 Mathematics and computer sciences [mathematics and other allied fields: computer sciences and other allied subjects (software development only; hardware development should be classified in the engineering fields)]
- 1.2 Physical sciences (astronomy and space sciences, physics and other allied subjects)
- 1.3 Chemical sciences (chemistry, other allied subjects)
- 1.4 Earth and related environmental sciences (geology, geophysics, mineralogy, physical geography and other geosciences, meteorology and other atmospheric sciences including climatic research, oceanography, vulcanology, palaeoecology, other allied sciences)
- 1.5 Biological sciences (biology, botany, bacteriology, microbiology, zoology, entomology, genetics, biochemistry, biophysics, other allied sciences, excluding clinical and veterinary sciences)

### 2. ENGINEERING AND TECHNOLOGY

- 2.1 Civil engineering (architecture engineering, building science and engineering, construction engineering, municipal and structural engineering and other allied subjects)
- 2.2 Electrical engineering, electronics [electrical engineering, electronics, communication engineering and systems, computer engineering (hardware only) and other allied subjects]
- 2.3. Other engineering sciences (such as chemical, aeronautical and space, mechanical, metallurgical and materials engineering, and their specialised subdivisions; forest products; applied sciences such as geodesy, industrial chemistry, etc.; the science and technology of food production; specialised



technologies of interdisciplinary fields, e.g. systems analysis, metallurgy, mining, textile technology and other applied subjects)

### 3. MEDICAL SCIENCES

- 3.1 Basic medicine (anatomy, cytology, physiology, genetics, pharmacy, pharmacology, toxicology, immunology and immunohaematology, clinical chemistry, clinical microbiology, pathology)
- 3.2 Clinical medicine (anaesthesiology, paediatrics, obstetrics and gynaecology, internal medicine, surgery, dentistry, neurology, psychiatry, radiology, therapeutics, otorhinolaryngology, ophthalmology)
- 3.3 Health sciences (public health services, social medicine, hygiene, nursing, epidemiology)

### 4. AGRICULTURAL SCIENCES

- 4.1 Agriculture, forestry, fisheries and allied sciences (agronomy, animal husbandry, fisheries, forestry, horticulture, other allied subjects)
- 4.2 Veterinary medicine

### 5. SOCIAL SCIENCES

- 5.1 Psychology
- 5.2 Economics
- 5.3 Educational sciences (education and training and other allied subjects)
- 5.4 Other social sciences [anthropology (social and cultural) and ethnology, demography, geography (human, economic and social), town and country planning, management, law, linguistics, political sciences, sociology, organisation and methods, miscellaneous social sciences and interdisciplinary, methodological and historical S1T activities relating to subjects in this group. Physical anthropology, physical geography and psychophysiology should normally be classified with the natural sciences].

### 6. HUMANITIES

- 6.1 History (history, prehistory and history, together with auxiliary historical disciplines such as archaeology, numismatics, palaeography, genealogy, etc.)
- 6.2 Languages and literature (ancient and modern)
- 6.3 Other humanities [philosophy (including the history of science and technology) arts, history of art, art criticism, painting, sculpture, musicology, dramatic art excluding artistic "research" of any kind, religion, theology, other fields and subjects pertaining to the humanities, methodological, historical and other S1T activities relating to the subjects in this group]

## 5. Address of the project public website and relevant contact details.

VIBRANT public website: [www.fp7-vibrant.eu](http://www.fp7-vibrant.eu)

### VIBRANT Principal Investigators

Principal Investigators	Institution	Partner	Short name	Contact
<b>Theo Schotten</b> (Coordinator), <b>Katja Werner</b> , Silke Johanning, Marieke Dieckmann, <b>Jan Niehaus</b> , Thomas Frahm, Maria Kappler, Carsten Ott	Center for Applied Nanotechnology (CAN) GmbH	1	CAN	<a href="mailto:ts@can-hamburg.de">ts@can-hamburg.de</a> <a href="mailto:kw@can-hamburg.de">kw@can-hamburg.de</a> <a href="mailto:jsn@can-hamburg.de">jsn@can-hamburg.de</a>
<b>Horst Weller</b> , Soeren Becker, Christian Schmidtke, Anna Kreuziger, Hauke Kloust, Michaela Steuter, <b>Joachim Thiem</b> , Julian Thimm, Daniel Waschke, Yevgeniy Leshch, Anna Jacobsen	Dept. of Chemistry, Univ. Hamburg	2	UH	<a href="mailto:weller@chemie.uni-hamburg.de">weller@chemie.uni-hamburg.de</a> <a href="mailto:thiem@chemie.uni-hamburg.de">thiem@chemie.uni-hamburg.de</a>
<b>Per-Olof Berggren</b> <b>Ingo Leibiger</b> , Barbara Leibiger, Sergej Zaitzev, Erwin Ilegems, Martin Kohler, Thusitha Paluwatte	Rolf Luft Research Center for Diabetes and Endocrinology, Karolinska Institutet Stockholm	4	KI	<a href="mailto:per-olof.berggren@ki.se">per-olof.berggren@ki.se</a> <a href="mailto:Ingo.Leibiger@ki.se">Ingo.Leibiger@ki.se</a>

<b><u>Abdullah Sener</u></b> , Karim Louchami, Sibel Cetik <b><u>Willy Malaisse</u></b> , Ying Zhang , Myrna Virreira	Laboratory of Experimental Hormonology, Brussels Free University	5	ULB	<a href="mailto:abdsener@ulb.ac.be">abdsener@ulb.ac.be</a> <a href="mailto:malaisse@ulb.ac.be">malaisse@ulb.ac.be</a>
<b><u>Ulf Ahlgren</u></b> , Maria Eriksson, Anna Eriksson	Centre for Molecular Medicine, Umeå University	6	UMU	<a href="mailto:ulf.ahlgren@ucmm.umu.se">ulf.ahlgren@ucmm.umu.se</a> <a href="mailto:maria.eriksson@ucmm.umu.se">maria.eriksson@ucmm.umu.se</a>
<b><u>James Sharpe</u></b> , Juergen Mayer, Jim Swoger	Centre for Genomic Regulation, Barcelona	7	CRG	<a href="mailto:James.Sharpe@crg.eu">James.Sharpe@crg.eu</a> <a href="mailto:juergen.mayer@crg.eu">juergen.mayer@crg.eu</a>
<b><u>Uwe Himmelreich</u></b> , Sonu Sharma, Greetje Vande Velde, Ashwini Ketkar-Atre, J.Raman Rangarajan, Ting Yin,	Katholieke Universiteit Leuven	9	K.U.Leuven	<a href="mailto:Uwe.Himmelreich@med.kuleuven.be">Uwe.Himmelreich@med.kuleuven.be</a>
<b><u>Kathrin Maedler</u></b> <b><u>Ekkehart Küstermann</u></b> , Anke Meyer	Centre for Biomolecular Interactions Bremen	10	UniHB	<a href="mailto:kmaedler@uni-bremen.de">kmaedler@uni-bremen.de</a> <a href="mailto:ekke@uni-bremen.de">ekke@uni-bremen.de</a>
<b><u>Stefan Förster</u></b> , Jasmin Nitsche, Stephanie Domes Nonio Wolter, Maria Ritter, Sascha Ehlert	Universität Bayreuth	11	UBT	<a href="mailto:stephan.foerster@uni-bayreuth.de">stephan.foerster@uni-bayreuth.de</a>
<b><u>Thomas Mandrup-Poulsen</u></b> , <b><u>Dan Holmberg</u></b> , Guy Novotny, Anja Schmidt-Christensen	Københavns Universitet	12	UCPH	<a href="mailto:tppo@sund.ku.dk">tppo@sund.ku.dk</a> <a href="mailto:dho@sund.ku.dk">dho@sund.ku.dk</a>

## 2. FINAL REPORT ON THE DISTRIBUTION OF THE EUROPEAN UNION FINANCIAL CONTRIBUTION

---

This report shall be submitted to the Commission within 30 days after receipt of the final payment of the European Union financial contribution.

### Report on the distribution of the European Union financial contribution between beneficiaries

Name of beneficiary	Final amount of EU contribution per beneficiary in Euros
1.	
2.	
n	
Total	

### References

- 
- <sup>1</sup> Speier et al., Nature Medicine, 2008, 14, 574 – 578.
- <sup>2</sup> Niehaus JS et al., patent application [WO2009101091 A1](#)
- <sup>3</sup> <http://www.can-hamburg.de/english/menu/products/candots-series-a.html>
- <sup>4</sup> [http://www.strem.com/uploads/web\\_structures/48-1011.gif](http://www.strem.com/uploads/web_structures/48-1011.gif)
- <sup>5</sup> Ran C, et al., Angew. Chem. Int. Ed. 2007, 46, 8998-9001.
- <sup>6</sup> Leclercq-Meyer V, Kadiata MM, Malaisse WJ; Int J Mol Med. 2000,6(2),143-52.
- <sup>7</sup> Ueberberg S et al., Diabetes October 2009, 58 (10), 2324-2334
- <sup>8</sup> a) Poeselt E, Kloust H et al., patent application EP2585210, b) Kloust H et al. Langmuir 2012, 28, 7276-7281, c) *ibid*, 2013, 29 (15), 4915–4921).
- <sup>9</sup> Malaisse WJ, et al. Arch Biochem Biophys. 2012 Jan 15;517(2):138-43
- <sup>10</sup> Thiem J et al., patent application WO2012016935A1.
- <sup>11</sup> Kloust H, et al., J. Phys. Chem. (manuscript submitted)
- <sup>12</sup> Malaisse WJ et al., Met Funct Res Diab, 2013, (Online) Vol 6, 1-5
- <sup>13</sup> a) Lundh M, Christensen DP, Rasmussen DN, Mascagni P, Dinarello CA, et al. Diabetologia (2010) 53, 2569-2578. b) Mandrup-Poulsen T, Pickersgill L, Donath MY; Nat Rev Endocrinol (2010) 6, 158-166. c) Lewis EC, Blaabjerg L, Storling J, Ronn SG, Mascagni P, et al. Mol Med (2011) 17, 369-377. d) Ablamunits V, Henegariu O, Hansen JB, Opare-Addo L, Preston-Hurlburt P, et al. Diabetes (2012) 61, 145-154. e) Cavelti-Weder C, Babians-Brunner A, Keller C, Stahel MA, Kurz-Levin M, et al. Diabetes Care (2012) 35, 1654-1662. f) Lundh M, Christensen DP, Damgaard Nielsen M, Richardson SJ, Dahllof MS, et al. Diabetologia (2012) 55, 2421-2431. g) Maedler K, Dharmadhikari G, Schumann DM, Storling J Handb Exp Pharmacol (2011), 257-278. h) Ardestani A, Sauter NS, Paroni F, Dharmadhikari G, Cho JH, et al. J Biol Chem. 2011; 286(19), 17144–17155. i) . Owyang AM, Maedler K, Gross L, Yin J, Esposito L, et al. Endocrinology. 2010, 151(6), 2515-27. j) Sauter NS, Schulthess FT, Galasso R, Castellani LW, Maedler K; Endocrinology 2008, 149, 2208-2218.
- <sup>14</sup> a) Haase A, Matthaei D, Bartkowski R, Duhmke E, Leibfritz D; J Comput Assist Tomogr (1989) 13, 1036-1040. b) Kustermann E, Meyer A, Godbole A, Dreher W, Maedler K; 19th Annual Meeting & Exhibition

---

International Society for Magnetic Resonance in Medicine (2010). c) Kustermann E, Meyer A, Godbole A, Dreher W, Maedler K; Proc Intl Soc Mag Reson Med 2011, 19, 810.

<sup>15</sup> Malaisse WJ, Maedler K; Diabetes Res Clin Pract. 2012, 98 (1), 11–18.

<sup>16</sup> Glas R, Sauter NS, Schulthess FT, Shu L, Oberholzer J, et al. Diabetologia 2009, 52, 1579-1588.

<sup>17</sup> Cheddad et al., IEEE Transactions on medical imaging, 2012

<sup>18</sup> Hörnblad A, Cheddad A, Ahlgren U; Islets 2011, 3, 204–208

<sup>19</sup> Eriksson AU, et al, *J. Vis. Exp.* (71), e50238, doi:10.3791/50238 (2013)

<sup>20</sup> Cheddad A et al., Optics Express, 2013, 21(14), 16584-604